2022

Stimulus coding over time in the hippocampus and prefrontal cortex

BOSTON UNIVERSITY

SCHOOL OF MEDICINE

Dissertation

STIMULUS CODING OVER TIME IN THE HIPPOCAMPUS AND PREFRONTAL CORTEX

by

CATHERINE MIKKELSEN

B.A., University of Notre Dame, 2012
B.S.M.E., University of Notre Dame, 2012

Submitted in partial fulfillment of the

requirements for the degree of

Doctor of Philosophy

2022

Approved by

First Reader

Marc Howard, Ph.D.
Professor of Psychological and Brain Sciences

Second Reader

Michael E. Hasselmo, D.Phil.
William Fairfield Warren Distinguished Professor
Professor of Psychological and Brain Sciences
Professor of Biomedical Engineering

DEDICATION

I would like to dedicate this work to United States Marines Corporal Nicholas Harris and Corporal Brandon Garabrant. Corporal Garabrant lived his life in service to others before making the ultimate sacrifice. His life and the desire to "Live a Life Worthy of Their Sacrifice" inspired me to pursue PTSD research as a means to help the ones who make it back home. Corporal Harris served two tours in Iraq and upon his homecoming showed us that in healing others we heal ourselves. He was incredible supporter throughout my graduate career, and his knowledge of the realities of combat and what it is like to be a combat veteran have immensely influenced my research. It was his insight into the impact of the constant stress surrounding combat trauma that inspired my inquiry into the impact of stress on generalization. He lived his life as a light for others and is deeply missed.

ACKNOWLEDGMENTS

I am thankful for the support of my friends and family in the pursuit of my research and degree. My parents, Dr. Edwin Mikkelsen and Karen Mikkelsen RN, have supported my interest in psychology and psychiatry from an early age, and have worked tirelessly to provide me with educational opportunities to pursue these interests. My sister, Dr. Kristen Unsicker has provided support and laughs along the way, as well as insight into applications of treatments. Their unconditional love and support has made possible everything I do.

I am grateful to Dr. Howard Eichenbaum for bringing me into the field of neuroscience, and for creating a lab environment in which helping each other succeed was encouraged and prioritized. I am thankful to my mentor Dr. Marc Howard, for teaching me not only how to be a careful and rigorous scientist, but also for teaching me to be a kind and effective teacher and mentor. I am thankful for my committee, Dr. Mike Hasselmo, Dr. Steve Ramirez, Dr. Zoran Tiganj, and Dr. Arash Yazdanbakhsh, for providing both scientific insights and for helping me develop the skills to communicate complex ideas. The GPN community, led by Dr. Shelley Russek and Dr. Sandi Grasso, has been a supportive group that has pushed me to think across academic "silos". I am eternally grateful for the fantastic people I have been fortunate to work in the lab with. Each has influenced my work and has allowed me to thrive by providing a supportive environment in which we all push for the success of others. Dr. Daniel Sheehan, Ariana Tortolani, and Blake Fordcye were instrumental in the behavioral work conducted in chapter 3.

STIMULUS CODING OVER TIME IN THE HIPPOCAMPUS AND PREFRONTAL CORTEX

CATHERINE MIKKELSEN

Boston University School of Medicine, 2022

Major Professor: Marc Howard, Professor of Psychological and Brain Sciences

ABSTRACT

The ability to create temporal relationships between stimuli is a critical component for both working and long term memory. Research has shown that the prefrontal cortex and the hippocampus are critical regions supporting the ability to create these "what and when" associations. This dissertation will use two methods to explore the connections between these associations: an analysis of previously recorded data to investigate the properties of time cells, and the development of a novel task to investigate the impact of valence on sequence learning.

Previous work has identified sequences of time cells that fire across a delay in response to a given stimulus. It is unknown how the presentation of subsequent stimuli affects these sequences. To interrogate this question, I utilized previously recorded extracellular data, originally published in Warden and Miller (2010), from the prefrontal cortex in monkeys performing working memory tasks. In these tasks, monkeys were presented with a list of two stimuli that they needed to remember to obtain a reward. Decoding analyses showed that information about the identity of a stimulus persists past the presentation of a second list item. Additionally, information about the time of the stimulus presentation is carried at the population level. Utilizing model fits of individual

cells, I identified subpopulations of cells that fire to time, stimulus and time, or list and time. I found that many "pure" time cells fire at similar times in both the first and second list position, but that some fire to what appears to be a conjunction of time and list position. Stimulus specific time cells often fire to a preferred stimulus regardless of which position it is presented. These results show that cells in the prefrontal cortex are able to encode a variety of task dimensions simultaneously.

Next, I developed a task to test the effect of valence on the encoding of "what and when". Typically, previous work has focused on the ability to associate neutral stimuli with either positive or negative stimuli. However, I sought to simultaneously interrogate positive and negative valences in the same task. In our task, rats were trained to discriminate four tones, of which two predicted a positive outcome, and two predicted a negative outcome. I was able to show that rats are able to learn the task. Learning was initially defined as the ability to perform two sessions in a given day above 80% accuracy, and can also be seen as a significant increase in the proportion of trials that were correct. This task could be used in future work to include cellular recordings and more complex behavioral manipulations, such as interrogating the effect of stress on generalization.

Overall, this work furthers the understanding of how the brain is able to associate stimuli across time to determine "what happened when".

TABLE OF CONTENTS

LIST OF FIGURES

LIST OF ABBREVIATIONS

AIC	Akaike Information Criterion
BIC	Bayes Information Criterion
CA1	Cornu Ammonis 1
CA2	Cornu Ammonis 2
CA3	Cornu Ammonis 3
CA4	Cornu Ammonis 4
DG	Dentate Gyrus
EC	Entorhinal Cortex
LDA	Linear Discriminant Analysis
MEC	Medial Entorhinal Cortex
PFC	Prefrontal Cortex
PTSD	Post- Traumatic Stress Disorder
TMS	Transcranial Magnetic Stimulation
TCN	Truncated Newton

CHAPTER ONE

Anatomical Review of the Prefrontal Cortex and Hippocampus

Anatomical connections yield insight into the ways information flows through the brain. What follows is a brief review of the anatomical connections within and between the prefrontal cortex and the hippocampus that will allow us to utilize common language when referring to sections of the brain across researchers as well as provide insight into how specialized regions relate to each other.

Prefrontal Cortex

The prefrontal cortex (PFC) is generally considered to comprise multiple subregions in the anterior part of the frontal lobe. However, controversy exists regarding the delineations and further in how to compare the prefrontal cortices of different species. This is especially true in contrasting primates and rodents. Identifying homologous regions typically takes into account factors such as cytoarchitectural similarity, connectivity, functional similarity, similarity in development, and representation of neurotransmitters in the area (Uylings et al., 2003).

Cytoarchtitecturally, the comparison between rodents and primates is difficult because in rodents the prefrontal areas are comprised entirely of agranular cortex, while it is comprised of granular cortex in primates (Öngür & Price, 2000). The prefrontal cortices are typically defined by their reciprocal connections with the mediodorsal nucleus of the thalamus (Uylings et al., 2003). In both rodents and primates, the prefrontal cortex is disynaptically connected to the hippocampus through nucleus reuniens of the thalamus and disynaptically through the entorhinal cortex (EC)

(Eichenbaum, 2017). The rodent prefrontal cortex is typically divided into the orbitofrontal cortex and the medial prefrontal cortex, with the medial prefrontal cortex further divided into the prelimbic and infralimbic cortices. In the primate brain, the prefrontal cortex is divided into the medial prefrontal, the orbitofrontal, and the dorsolateral prefrontal subregions. The lateral prefrontal cortex is often investigated in working memory tasks (Brincat & Miller, 2015; Cromer et al., 2010; Warden & Miller, 2010). It is commonly thought that the rodent does not possess a region analogous to the dorsolateral prefrontal cortex in the primate (Uylings et al., 2003).

Hippocampus

The hippocampus is located in the medial temporal lobe and is divided into a number of subregions. These subregions include the cornu ammonis 1 (CA1), cornu ammonis 2 (CA2), cornu ammonis 3 (CA3), cornu ammonis 4 (CA4), the dentate gyrus (DG) and subiculum. These areas are composed of multiple layers, including the stratum lacunosum, stratum radiatum, stratum pyramidale, stratum oriens, and the alveus. Within the hippocampus, DG projects to CA3 through the mossy fiber pathways. CA3 projects to CA1 through the Schaffer Collaterals. CA1 then projects to the subiculum (Amaral & Witter, 1989).

CA1 also has outputs to EC and nucleus reuniens. These are important connections for this work because they then form a disynaptic pathway to the prefrontal cortex. Information from the PFC then returns via a disynaptic pathway through EC (Eichenbaum, 2017). Within the medial temporal lobe, the amygdala projects to the

ventral portion of CA1. This projection is thought to be important for conveying salience information, particularly with regard to fear memories.

Representations of Space and Time in the Brain

There has been an understanding going back as far as Aristotle, that memories contain important dimensions of when, where, and what happened. In the centuries since, efforts have undertaken the discovery of how these properties are encoded in the brains to create the experience of memories, including the utilization of cells that specifically encode for these variables (Eichenbaum, 2013).

Place Cells Encode Spatial Location

Place cells fire consistently in a particular location (O'Keefe & Dostrovsky, 1971; O'Keefe & Burgess, 2005). In a linear environment, their field width expands with distance from the start location (Sheehan et al., 2021). While many studies of place cells have occurred in relatively small environments (dimensions not exceeding 1-2 meters), recent developments in recording technology have allowed researchers to examine their properties over larger distances. These experiments have shown that place cells can have multiple fields of varying sizes (Eliav et al., 2021; Fenton et al., 2008; Rich et al., 2014). Additionally, many place cells will "remap", or drastically change their firing location, after changes to the environment (Kinsky et al., 2018; Muller & Kubie, 1987).

Time Cells Encode Temporal Information

Time cells, or episode cells, are similar to place cells in that they tile a continuous dimension, but differ in that the field is temporal instead of spatial. Time cells were first reported in a study by Pastalkova et al. (2008), in which rats were trained to perform a delayed alternation task with a running wheel on the center stem. They found that despite being fixed in place, cells fired at distinct and punctate epochs during the delay. The tendency of time field widths to increase with distance from an initial stimulus also parallels spatial work (Cao et al., 2021; Cruzado et al., 2020; Howard et al., 2014; Kraus et al., 2013; Sheehan et al., 2021). These time cells have been identified repeatedly since their initial discovery (Kraus, 2015; Kraus et al., 2013; MacDonald et al., 2011; MacDonald et al., 2013; Robinson et al., 2017; Mau et al., 2018). While some of these cells may be encoding distance run, others fire at a consistent time despite changes to running speed, and therefore distance run during that time (Kraus et al., 2013). In other experiments, a head-fixed preparation was utilized, removing any possibility that they are solely a spatial confound (Cruzado et al., 2020; Goh, 2022; MacDonald et al., 2013; Taxidis et al., 2020; Tiganj et al., 2019).

Time cells have been found in other regions and species. Other hippocampal subregions with time cells include CA3 (Salz et al., 2016), and DG (Goh, 2022). They have also been found in the rodent prefrontal cortex (Tiganj et al., 2017), MEC (Kraus et al., 2015), and striatum (Akhlaghpour et al., 2016; Mello et al., 2015). In primates, time cells have been found in the hippocampus (Cruzado et al., 2020; Gill et al., 2011;

Umbach et al., 2020), and the prefrontal cortex (Cruzado et al., 2020; Jin et al., 2009; Tiganj et al., 2018), and striatum (Jin et al., 2009).

Time cells have been found in an expanding number of tasks. Much of the original work focused on delayed alternation (Kraus et al., 2013; Pastalkova et al., 2008). Since then, many studies have utilized versions of delayed match to sample(Cao et al., 2021; Cruzado et al., 2020; MacDonald et al., 2013; Taxidis et al., 2020; Terada et al., 2017). Time cells have also been found in a task where monkeys were asked to make categorical distinctions of presented stimuli (Tiganj et al., 2018). These tasks with specific stimuli have shown that some time cells show conjunctive representations of stimulus and temporal information (Cruzado et al., 2020; Tiganj et al., 2018). However, to date no studies have shown the effect of multiple stimuli. Finally, rats recorded in a looping task with a delay, show that time cells do not require a cognitive load to fire (Goh, 2022; Mau et al., 2018; Salz et al., 2016).

Time Cells Offer a Way to Store Information in a Scale Invariant Manner

Previous sections have touched on the observation that the width of time cell fields tend to increase as the cells move further into the trial. This correlation has many significant theoretical underpinnings, and allows for scale invariance (Howard et al., 2014). The chaining model has been proposed as a method by which temporal associations could be formed. However, this would require linearly increasing numbers of cells for increasing time periods (Eichenbaum, 2013). By utilizing logarithmic compression, time cell fields allow for increasing time to be encoded at a lower computational cost, which is also scale invariant (Cao et al., 2021). This finding parallels

that of the Weber-Fechner law in psychophysics that shows that variability increases with increasing number (Fechner et al., 1966). Previous work (Cao et al., 2021; Cruzado et al., 2020; Howard et al., 2014) has shown a linear relationship between time within trial and field width for time cells across a single delay.

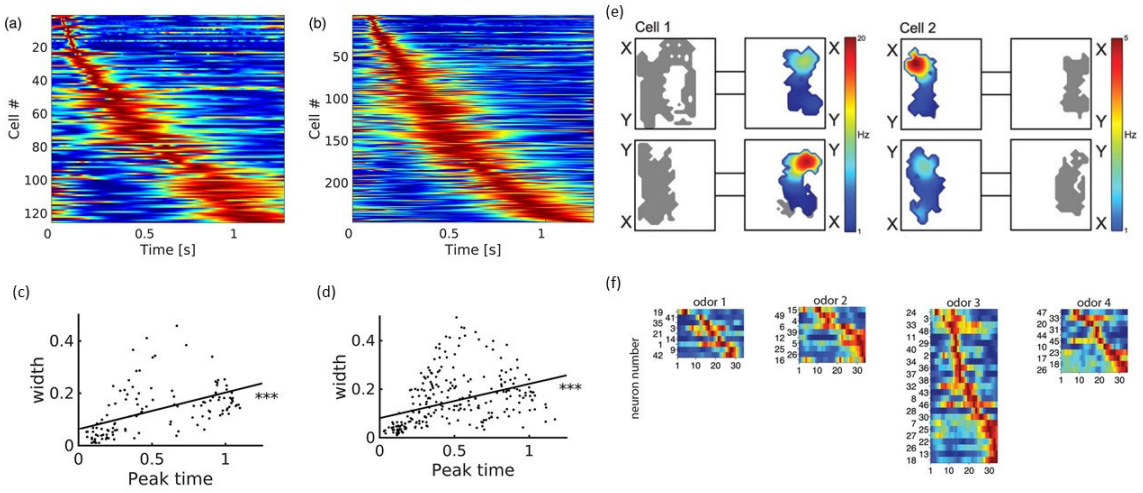

Figure 1.1: Examples of temporal firing and mixed selectivity in the literature. a-b) Heatmaps of time cells in the primate hippocampus (a), and prefrontal cortex (b), show distinct time fields tiling the entirety of the delay (Cruzado et al., 2020). c-d) The width of these fields increases with increasing peak time of the cells in the hippocampus (c) and prefrontal cortex (d) (Cruzado et al., 2020). e) Hippocampal cells in rats show conjunctive encoding. Fields represent the behavioral apparatus, with object identities noted (X and Y) for separate trials. Cells show mixed selectivity in the form of increased firing to a preferred stimulus in a particular location. (Komorowski et al., 2009, Copyright Society for Neuroscience, 2009) f) Time cells in rats show mixed selectivity. Time cells fire in distinct sequences to each of the four odors presented in the task. (MacDonald et al., 2013)

Computational models of human list learning behavior include chaining, in which items in a list are related to the items next to them (Henson, 1998). This parallels the theory of chaining in neurons, in which firing of one neuron cues firing of the next neuron in a sequence (Eichenbaum, 2014). This contrasts models of ordinal theory, in

which elements are associated with a “node” on a continuous dimension, and the elements are not directly associated with each other (Henson, 1998). This theory parallels theories of time cells as a product of the temporal context cells in which they are associated (Eichenbaum, 2014; Howard et al., 2014).

Mixed Selectivity Across Dimensions

Mixed selectivity presents an opportunity for cells to encode multiple dimensions of a task simultaneously. The ability of neurons to fire to combinations of tasks demands allows for a linear readout in downstream areas, as well as allowing for the brain to engage in increasingly complex tasks without needing ever increasing numbers of neurons (Fusi et al., 2016; Rigotti et al., 2013). Of note, the selectivity of these neurons can be seen as context dependent, with the same neurons participating in different ensembles for different tasks (Fusi et al., 2016). In the hippocampus, some have proposed that place cells firing in an open field environment in fact represent conjunctive encoding of distance from available landmarks (O’Keefe & Burgess, 1996). In other regions, such as the retrosplenial cortex, egocentric boundary cells can be seen as representing the conjunctive positions of the animal and an object or wall (Alexander et al., 2020). Combining across modalities, mixed selectivity can be seen in the conjunctive encoding of spatial and object information (Komorowski et al., 2009). Throughout the temporal lobe, spatial and object information can also combine with more abstract dimensions such as context (Farovik et al., 2015; Keene et al., 2016; Komorowski et al., 2013; McKenzie et al., 2014).

Similarly, stimulus and temporal information are encoded simultaneously (Cruzado et al., 2020; MacDonald et al., 2013; Terada et al., 2017; Tiganj et al., 2018). This takes the form of stimulus-specific time cells, which fire at a particular period during the delay, but primarily after a specific stimulus is presented. This mixing is advantageous for the population as a whole as the number of dimensions increases (Fusi et al., 2016; Rigotti et al., 2013).

The Impact of Valence on Memory

An additional axis that we can consider that is encoded in our memories is that of valence. The valence axis spans from positive to neutral to negative. The valence of a memory impacts the extent to which it is stored in long term memory and the mechanisms which are used to encode it.

Salience Impacts Neuronal Representation

Previous work has shown that dorsal CA1 coding can be influenced by the valence of the stimuli. Early work showed an increased density of place fields at the platform location in a water maze task, even when the platform was removed (Hollup et al., 2001). This distinction is important as some cells code specifically for reward across locations and environments (Gauthier & Tank, 2018). When these cells are optogenetically activated away from the reward location, rats demonstrate increases in licking behavior associated with reward (Robinson et al., 2020). Furthermore, the stability of the place code is influenced by the engagement of the animal in the task

(Kentros et al., 2004), and temporal fields are more precise in tasks which require temporal information to solve them (Cueva et al., 2020).

With regard to negative stimuli, animals show increased representation and reactivation of an "air puff zone" as compared to the rest of the linear track (Girardeau et al., 2017). Finally, investigations of the simultaneous representations of positive and negative memories in ventral CA1 have shown that populations of cells may represent events of similar valence, but do not remap onto opposing valences (Shpokayte et al., 2020). Outside the hippocampus in the amygdala, neurons show increased generalization with increased shock intensity (Ghosh & Chattarji, 2014).

Memory in Disease

In parallel with our understanding of how neurons encode dimensions of memory, research has also investigated how neurological, psychiatric and psychological diseases effect these processes. Reduced hippocampal volume has been correlated with diseases like Post Traumatic Stress Disorder (PTSD) (Gilbertson et al., 2002), Alzheimer's Disease, and its predecessor mild cognitive impairment (De Santi et al., 2001) , Parksinson's Disease (Xu et al., 2020). In PTSD the smaller hippocampal volume may be a risk factor in the development of PTSD following exposure to trauma (Gilbertson et al., 2002).

Animal models of memory are used to understand the mechanisms that underlie many of these diseases. In humans, exposure to traumatic experiences can lead to PTSD, which can include generalization of fear responses to neutral stimuli, avoidance of triggering stimuli, sleep disturbances, and "flash-backs" or realistic reliving of the

experience. Treatment for PTSD often includes exposure therapy, or retelling of the event in a safe environment. This is largely based off of extinction training in animals who have undergone fear conditioning paradigms. Contextual and trace fear conditioning are the most common fear conditioning paradigms (Phillips & LeDoux, 1992). In contextual fear conditioning animals are exposed to a context and then a shock is applied. In trace fear conditioning, a discrete event such as the playing of a tone proceeds an aversive event at a given delay. Single Prolonged Stress has also been developed to model PTSD behaviors in rodents. In this paradigm animals first undergo a 2-hour restraint, followed by a 20-minute group forced swim, and then exposure to ether. Finally, they are isolated from other animals in their home cage for at least 7 days (Liberzon et al., 1997). Social defeat can be used to model PTSD and depression. In this paradigm C57 mice, an ordinary laboratory breed, are exposed to highly aggressive CD1 mice for a prolonged period of time (Golden et al., 2011).

These behavioral paradigms are essential for furthering our understanding of how animals, from rodents to humans, encode highly salient and traumatic memories. The knowledge of the biological underpinnings of these phenomenon can be utilized to improve treatments, such as the use of pharmacological intervention (Haider et al., 2020), or behavioral therapies (Dunsmoor et al., 2015).

Exposure therapy has become a popular therapeutic approach for anxiety disorders, based off of extinction in fear conditioning, and efforts have continued to explore mechanisms that can increase its efficacy, or decrease the number of sessions required (LeDoux, 2015). For example, changes to behavioral paradigms include

reconsolidation update (Schiller et al., 2010), the effect of early intervention (Yehuda & LeDoux, 2007), the effect of social interactions (Finkelstein et al., 2022), and investigations into the effect of stress on extinction training (Miracle et al., 2006).

Optogenetic investigations into the mechanisms of traumatic experience have yielded useful information. For example, activation of a fear "engram" in the dentate gyrus in a neutral context is sufficient to drive fear behavior (Liu et al., 2012; Ramirez et al., 2013), and activation of positive memories decreases depressive behavior (Ramirez et al., 2015). Subsequent work has shown the ability to modulate emotional memory across the positive-negative divide (Redondo et al., 2014). While optogenetic manipulation is not currently a tractable treatment for humans, increasing our knowledge of how specific brain regions and pathways participate in the extinction process can help to guide the development of treatments such as the use of transcranial magnetic stimulation (TMS) in combination with exposure therapy (Isserles et al., 2021; Lantrip, 2021). For further review on the implications of animal work on treatment of pathologies see Denny et al. (2017) .

CHAPTER TWO[1]

Introduction

The prefrontal cortex has long been implicated in working memory (Fuster & Alexander, 1971; Goldman-Rakic, 1995; Jacobsen, 1936; Miller & Cohen, 2001). Cognitive models of working memory require multiple past stimuli to be represented in working memory (Atkinson & Shiffrin, 1968; Baddeley & Hitch, 1974); this is necessary to allow associations to be formed between stimuli for later recall (Kahana, 1996). Although early work focused on content-specific persistent firing of neurons in PFC as a neural model for working memory (Funahashi et al., 1989; Miller et al., 1991), more recent neurophysiological work studying firing of PFC neurons has identified more subtle and complex signatures of firing associated with maintenance of information in working memory (Lundqvist et al., 2018). This paper focuses on how information about multiple past items, and the time at which they were presented, are expressed in the firing rates of neurons in PFC using a canonical dataset (Warden & Miller, 2010).

Non-linear mixed selectivity in PFC ensembles

Consider stimuli that differ on multiple dimensions. For concreteness, let us consider two visual shapes, square or circle, and two different colors, red and blue. Content-specific firing for these shapes could be divided among the different features.

[1] This chapter is based on a paper that has been submitted for publication entitled "Coding of time with non-linear mixed selectivity in Prefrontal Cortex Ensembles" Authors: Catherine A. Mikkelsen, Stephen J. Charczynski, Scott K. Brincat, Melissa R. Warden, Earl L. Miller, Marc W. Howard

For instance, some neurons might fire to circles, regardless of their color, while other neurons fire to squares, regardless of color. Another separate population could fire only to the color of the stimuli, and ignore the shape. In contrast, one could imagine a population where many neurons fire to conjunctions of stimuli. For instance, one neuron might fire only for red circles and fire for neither red squares nor blue circles. This form of coding is referred to as non-linear mixed selectivity. Rigotti et al., (2013) observed that firing in the PFC during maintenance of information in working memory for short lists included many conjunctive neurons that coded for features extended in time, such as neurons that coded for a particular stimulus in a particular serial position. Non-linear mixed selectivity endows a system with many computational advantages, at the cost of requiring many more neurons to cover the stimulus space than would have been necessary for neurons that only coded for one or another feature (Fusi et al., 2016; Sreenivasan & D'Esposito, 2019). Mixed selectivity in the prefrontal cortex may also be a reflection of the top-down influence of attention on primary cortices (Sreenivasan et al., 2014). The utility of non-linear mixed selectivity is supported by the finding that conjunctive coding is also observed in the hippocampus, for a wide range of variables (Anderson & Jeffery, 2003; Komorowski et al., 2009; Nieh et al., 2021; Wood et al., 2000; Wood et al., 1999). Indeed, the fact that hippocampal place cells exhibit radial basis functions for position has long been argued to reflect conjunctive coding for distance to different landmarks available in an environment (O'Keefe & Burgess, 1996).

Timing Information in PFC ensembles.

Representations of the time at which items were experienced has long been an important feature of cognitive models of working memory (Brown et al., 2000; Hacker, 1980; Howard et al., 2015). In the last decade, a growing body of work has demonstrated that the firing of neurons in a wide range of brain regions carry information about the time at which past events were experienced (Kraus et al., 2013, 2015; MacDonald et al., 2011; Mau et al., 2018; Mello et al., 2015; Rossi-Pool et al., 2019; Tsao et al., 2018). In the hippocampus, sequentially-activated time cells (MacDonald et al., 2011; Pastalkova et al., 2008) can be used to reconstruct the time since a delay interval began. Because different stimuli in a working memory experiment trigger distinct sequences, hippocampal time cells can be understood as conjunctively coding for what happened when in the past (Cruzado et al., 2020; Taxidis et al., 2020; Terada et al., 2017). The same type of conjunctive coding of what happened when in the past can be observed in sequentially-firing neurons in PFC (Cruzado et al., 2020; Tiganj et al., 2018). Sequentially-activated time cells are not the only way a neural population may code for the time of past events. For instance, in entorhinal cortex, time can be decoded from populations of neurons that change their firing monotonically over time, but at a wide variety of rates (Bright et al., 2020; Tsao et al., 2018). Indeed, many authors have noted that the firing of PFC neurons carries information about time while not explicitly describing sequential firing (Cavanagh et al., 2018; Cueva et al., 2020; Murray et al., 2017).

Temporal Mixed Selectivity in lists of multiple items.

Prior work has established that prefrontal neurons use non-linear mixed selectivity to code for information maintained in working memory after a brief list. Prior work has also established that sequentially-activated neurons code for time by tiling the delay following a stimulus, showing conjunctive coding of what happened when. However, previous work on timing information has focused on delays following a single item (but see Goh, 2022). This leads to a critical question. As the number of items in a list grows, the number of neurons necessary to conjunctively code for the list grows exponentially (the number of lists composed of N items of length L goes like N^L). This concern becomes more acute if the ensemble also retains information about the time of each of the separate items in the list. In this paper we study the retention of information in working memory during study of short lists of visual stimuli using an existing dataset (Warden & Miller, 2010). The primary question is how information about the time and identity of earlier items is retained following the presentation of the second item in the list.

Methods

Description of Behavioral Task

Warden & Miller (2010) trained two monkeys to remember lists of two visual stimuli. Each of the four clearly distinguishable images could appear in either list position. The same stimulus could not appear twice in the same list. Each stimulus was presented for 500ms with a 1s delay after each presentation. For this paper, only the time of list presentation, or the first 3000ms of each trial, was considered. After each list, the

animals were presented with one of two behavioral decision tasks that required the monkey to remember the list. The data from both tasks was combined. Recordings were made in the prefrontal cortex. See Warden and Miller (2010) for complete methods.

Population Analyses

Our primary interest is to know how the firing of PFC neurons after the second list item was presented reflected memory for the first list item. To evaluate this, we will attempt to decode the stimulus in the first serial position at all points during presentation of the list. As a control, we will attempt to decode the stimulus in the second serial position at all time points during list presentation. Decoding accuracy of the second list item prior to the time it was presented provides a baseline that controls for dependencies between the serial positions and any other methodological issues that may arise from the decoder.

A cross temporal classifier was used to identify stimuli based on neural firing data. This involves running a linear discriminant analysis for all of the combinations of time bins. The classifier was trained to decode the stimulus on each trial using firing from a given time bin and then tested on firing from all time bins. The linear discriminant analysis (LDA) uses firing rate averaged over each bin on each training trial to create a linear model, for which each neuron is a variable. Firing on a separate set of test trials is then evaluated by the model to predict the probability of the stimulus identities for the test trials. We implemented the classifier using the Matlab function “classify”. Random normally distributed noise was added to the training and test data with a sigma of 10^{-7} and a mu of 0, in order to prevent singularities.

We sought to decode the identities of the stimuli presented in both presentation positions. Firing was divided into 250ms blocks. Each run contained 260 training trials, 40 test trials, and 200 units. Units were selected that have at least 420 trials (1.4 x (training trials + test trials)). 50 repetitions were run of this analysis and the average accuracies were calculated. Each repetition contained 200 randomly selected units. We compared the bins representing equal offset for the classification of the second stimulus after the presentation of the first, and the classification of the first stimulus after the presentation of the second. For example, we compared classification of stimulus 1 at 2000 ms (500 ms after the other item was presented) to classification of stimulus 2 at 500ms (500 ms after the other item was presented).

We also sought to decode time to determine if temporal information persists throughout the entirety of the trial. We again used a linear discriminant analysis, but divided the trial into ten 300ms bins. The classification of time bin used 200 training trials and 60 test trials. Units were included that had at least 312 trials (1.2 x (training trials + test trials)). We used 150 randomly selected units for each repetition instead of 200 due to the differences in number of trials needed for the increase in the number of outcomes.

Analysis of Individual Cells

We sought to characterize the firing field of each neuron using a series of models that were fit to the spiking profile. We included four models: a constant model, a ``pure time" model with Gaussian receptive fields, a stimulus-specific time cell model, and a conjunctive time cell model. Parameters for each model were selected to maximize the

likelihood of the observed spike train across sequences. While the Gaussian time field model does not capture the nuances of the firing fields, the representation is sufficient to identify cells whose firing is modulated by the stimulus identity and temporal patterns.

First, we identify all time cells. To do this we compare the log likelihoods of the model fits for the Gaussian model to the constant model. Next the time cells are divided into three mutually exclusive subpopulations: pure time cells, stimulus-specific time cells, and conjunctive time cells. “Pure” time cells are those whose fit was not improved by adding parameters sensitive to the stimuli presented on each trial. The stimulus-specific model has four separate stimulus parameters in addition to the parameters of its time field. The conjunctive model has 12 parameters one for each possible list (recall that the four stimuli were never repeated within a list). The stimulus-specific time cells are defined as those for which the stimulus-specific model is a better fit than the Gaussian and conjunctive models. The conjunctive time cells are defined as those for which the conjunctive model is a better fit than the Gaussian and stimulus-specific models.

Model fits and parameter selection were performed on the cells using a customized program Maxlikespy (*GitHub - tcnlab/maxlikespy*, n.d.), which utilizes scipy’s basin-hopping method to determine model parameters. This method is similar to previous work (Cruzado et al., 2020; Tiganj et al., 2018). The basin hopping algorithm was run until a better fit could not be found for 1500 iterations. It uses the Truncated Newton (TCN) method as the minimization method. The first model simply estimated a constant firing rate:

$$p(t;\theta) = a_0$$

The ``pure time'' model adds a Gaussian temporal receptive field:

$$p(t;\theta) = a_0 + a_1[T(t;\mu,\sigma) + T(t-1500;\mu,\sigma)]$$

where

$$T(t;\mu,\sigma) = e^{\frac{-(t-\mu)^2}{2\sigma^2}}$$

The stimulus specific time cell model allows us to consider the influence of stimulus specificity on the firing of the neurons in addition to temporal specificity. It considers each of the four stimuli separately. For the stimulus specific Gaussian model, the value of c_{i1} was set to one for trials when the stimulus was presented in the first location, and c_{i2} was set to one for trials when the stimulus was presented in the second location.

$$p(t;\theta) = a_0 + \sum_{i=1}^{4} a_i c_{i1} T(t;\mu,\sigma) + a_i c_{i2} T((t-1500);\mu,\sigma)$$

The conjunctive time cell model has separate information about the identities of the stimuli in the first and second presentations. For the conjunctive model the value of c_i

was set to one for trials when the associated list was presented (ie. both stimuli in order), and zero for all other lists.

$$p(t;\theta) = a_0 + \sum_{i=1}^{12} a_i c_i [T(t;\mu,\sigma) + T((t-1500);\mu,\sigma)]$$

For all temporal models, the model fits are able to account for two peaks in a cell's firing that are 1500 ms apart. The mu value was allowed to vary from 0 to 3000ms. Sigma is allowed to vary from 0.001 to 1000ms. The coefficients are bounded such that the sum of all a's is less than 1. To correct for differing numbers of parameters we used the Matlab function "lratiotest" using a p-value of 0.01 (Bonferonni corrected). The constant model has one parameter, the pure time cell model has 4 parameters; the stimulus specific time cell model has 7 and the context-dependent stimulus specific time cell model has 15.

Prior work studying time fields following presentation of one item shows a monotonic, roughly linear, relationship between time field width and the peak time. Inspection of analogous plots for this dataset showed an apparent discontinuity after the second list item was presented at 1500 ms. To evaluate this hypothesis, we compared a regression of parameters over values of mu spanning the entire duration of the list (0 to 3000 ms) to a piecewise regression that fit the intervals 0 to 1500 ms and 1500 ms to 3000 ms separately. Each of these regressions used constant and linear terms. We compared the best-fitting model over the entire interval to the best-fitting piecewise

models using Akaike Information Criterion (AIC) and Bayes Information Criterion (BIC).

The stimulus classifier approach utilized for the entire population can be modified to be combined with the analyses of subpopulations of cells. For this analysis we analyzed only the bins for which training and testing are equivalent. Because of the decreased number of cells available, only 50 units were used per repetition. There were still 260 training trials and 40 test trials.

Results

Neural data can be used to classify "what" happened throughout the trial

A cross-temporal classifier was able to decode the identity of the first stimulus above chance even after the presentation of the second stimulus, as shown in Figure 1. The accuracy of the decoder decreases from 250ms until the presentation of the second stimulus ($p < 0.01$, slope= -2.5×10^{-4}). While the ability of the classifier to decode the identity of the first stimulus drops off over time, it did not return to chance after the presentation of the second stimulus. The box plot in Figure 1d shows the accuracy of the decoding of the first stimulus (blue) for all time points across the diagonal, as compared to the accuracy of the decoding of the second stimulus (black), for all time points across the diagonal. We used two tailed two-sample t-tests on the distributions of the classifier accuracies for a given set of parameters to compare these two epochs. For example, we can compare the decoding of stimulus 2 from 0-250 ms to the decoding of stimulus 1 from 1500-1750ms. Repeating this process, we find that each of these pairs

is significantly different ($p<0.01$). There are 98 degrees of freedom for all pairs. The t-statistics are, in order from stimulus onset, 11.9815, 9.7968, 10.2802, 11.5106, 10.3817, 12.5892.

The neural data can be used to classify "when" throughout the trial

Time can also be decoded from the neural data (Fig 2.1b). This shows that there is temporal information carried in the neural firing. If we count the number of classifications for each potential time bin, for each row, the distribution is significantly different than for a uniform distribution ($p<0.01$). We found that the distribution of the probabilities was significantly different from chance for each row using 10-sample test for given proportions x^2 (10) ranging from 169.4 to 585.8, all $p < .001$.

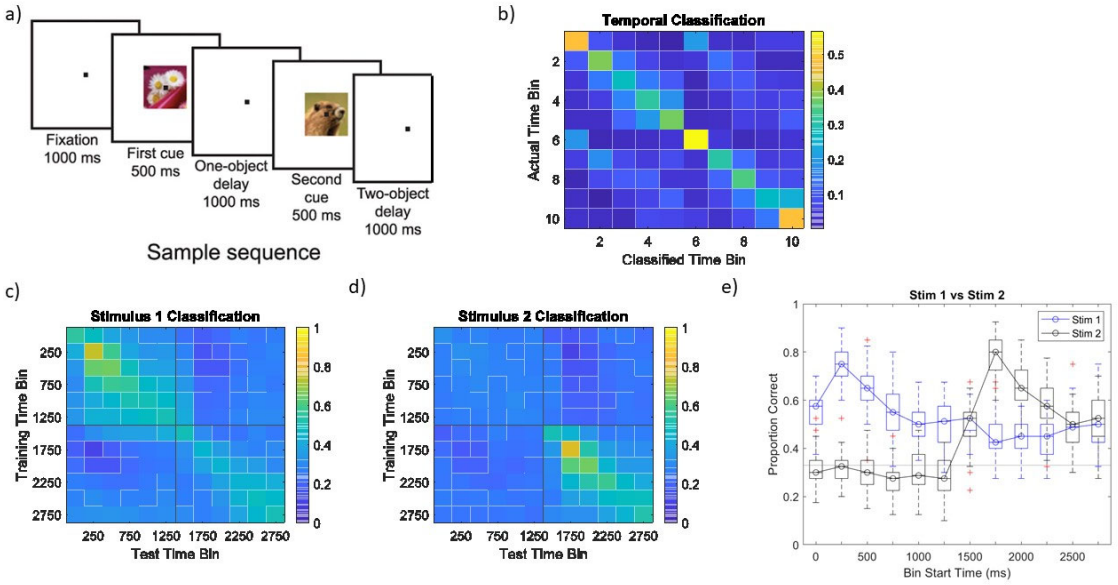

Figure 2.1: The population of neurons represents the identity and time of the first stimulus throughout the trial. a) A description of the task. The animal is presented with a stimulus from 0-500ms, followed by a delay from 500-1500ms. The second stimulus is presented from 1500-2000ms, followed by another delay from 2000-3000ms. b) A linear discriminant analysis (LDA) shows the ability to decode time bins. Each row represents the actual time bin for a set of decoded trials. The number of classified time bins for each row is counted and then normalize by the number of trials for the row. c) A cross temporal classifier is able to decode the identity of stimulus 1, even after the presentation of the second stimulus. d) A cross temporal classifier is able to decode the identity of the second stimulus, after it is presented at 1500ms. e) This graph shows the accuracy of the cross temporal classifier for when the training time bin and the test time bin are the same. The accuracy increases rapidly for stimulus 1 classification (blue) and then slowly drops off, but never to chance. The accuracy for stimulus 2 classification (black) increases after the presentation of the second stimulus at 1500ms.

Temporal parameters from model based analysis

The overwhelming majority of units, 792/867 were better fit by a model with a Gaussian time field than by the model with only constant firing rate. These 792 ``time cells" were further classified as 189 pure time cells, 367 stimulus-specific time cells, and 214 conjunctive time cells based on criteria described in the methods. We describe the properties of each of these groups below.

Pure Time Cells

Figure 2 summarizes the properties of the units classified as ``pure time cells''. These cells fire in a temporally modulated way irrespective of the stimulus presented. The heat map in figure 2.2a shows that many of these cells have two fields, equally distant from each stimulus presentation. However, there exists a subpopulation of cells (see red circle) that fire only after the presentation of the second stimulus. These cells may also be sensitive to serial position, and could also be successfully fit by a model that combines time with presentation period. Alternatively, they could be triggered by the first item, but at a delay longer than 1500 ms. However, these two possibilities are confounded due to the equal spacing on each trial.

We see a diversity of sigma and mu values (Fig 2.7) for this subpopulation. Investigating the relationship between the mu and sigma values, the best model fit was the split linear model (ΔAIC=27.8, ΔBIC = 21.3). The fact that the piecewise linear model was a better fit argues against the hypothesis that the cells with mu > 1500 ms reflect linearly increasing sequences initiated by the first stimulus.

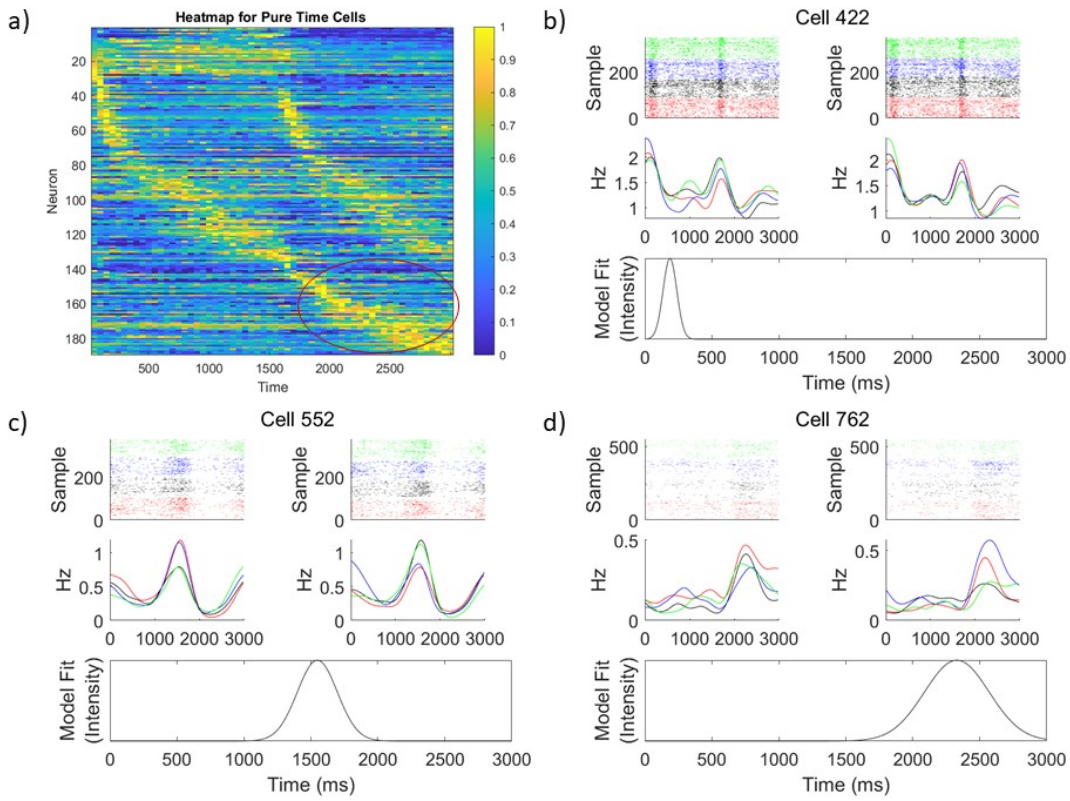

Figure 2.2: Single units best fit by the pure time model. a) A heat map of the pure time cells, sorted by the mu value of the Gaussian only model, shows cells that fire at a specific time, indifferent to the stimuli that are presented. Each row represents the self-normalized firing of each neuron. The cells circled in red show cells that fire to time only within the second presentation epoch. b-d) Rasters of time cells show punctate fields. Samples are color-coded and sorted by stimulus 1 identity on the left, and stimulus 2 identity on the right (trials where stimulus A is shown are in red, stimulus B in black, stimulus C in blue, and stimulus D in green). The top panel shows rasters where each row represents a trial, and each line marks times the cell fired within that trial. The second panel is the Gaussian smoothed firing rate, calculated separately for each stimulus identity. The bottom panel shows the model fit for the Gaussian model.

Stimulus Specific Time Cells

Stimulus specific time cells are the 367 cells for which the cell's firing is modulated by time and the stimulus-identity. Stimulus- specific time cells also tile the entirety of the trial, and cells responsive to a stimulus presented first may have temporal

fields after the presentation of the second stimulus. Shown in figure 3a, we note that there is a subpopulation of 31 cells that fire to a particular stimulus at a time greater than 1500ms (8.4% of stimulus selective cells), or after subsequent stimuli have been presented (red circle). Many of those cells firing before 1500ms fire at the same time point to either presentation period. Of note, while the cells fire in either position, firing is averaged across all trials, and the same stimulus is never presented twice in a trial. Therefore, it is impossible to tell if these cells would fire twice in a single trial given a trial with the same stimulus twice. Figure 2.4 shows heat maps broken out for each stimulus. Early and mid-trial examples of stimulus- specific time cells are shown in Figure 2.3b and 2.3c. Figure 2.3d shows an example of a stimulus-specific time cell with a late temporal field. Importantly, the heat map appears to terminate its “hook” at 1500ms.

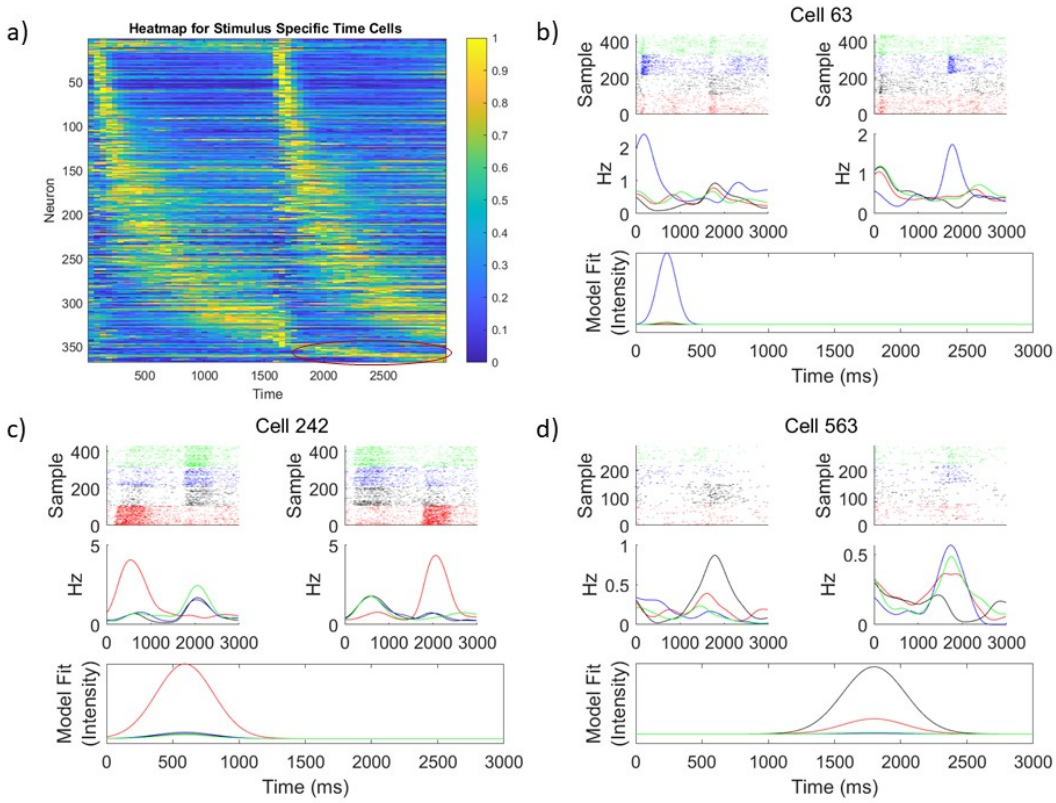

Figure 2.3: Single units best fit by the stimulus selective time cell model. a) A heat map shows that the stimulus-specific time cells tile the entirety of the delay with punctate fields. Each row represents the normalized firing of a neuron, and neurons are sorted by the model mu value of the conjunctive model fit. Firing is averaged across all trials. b-d) Examples of rasters for stimulus specific cells show punctate fields whose firing is modulated by stimulus identity, but typically regardless of the serial position in which the stimuli are presented. Trials are color-coded by and sorted by stimulus 1 identity on the left, and stimulus 2 identity on the right (trials where stimulus A are shown are in red, stimulus B in black, stimulus C in blue, and stimulus D in green.) Because the same stimulus is never shown twice in a trial, trials when the preferred stimulus is presented opposite the color code, a slight darkening appears to the other stimuli in the opposite position. The top panel shows rasters where each row represents a trial, and each line marks times the cell fired within that trial. The second panel is the Gaussian smoothed firing rate, calculated separately for each stimulus identity. The bottom panel shows the model fit of the stimulus specific model. This model shows firing for stimulus A in red, stimulus B in black, stimulus C in blue, and stimulus D in green.

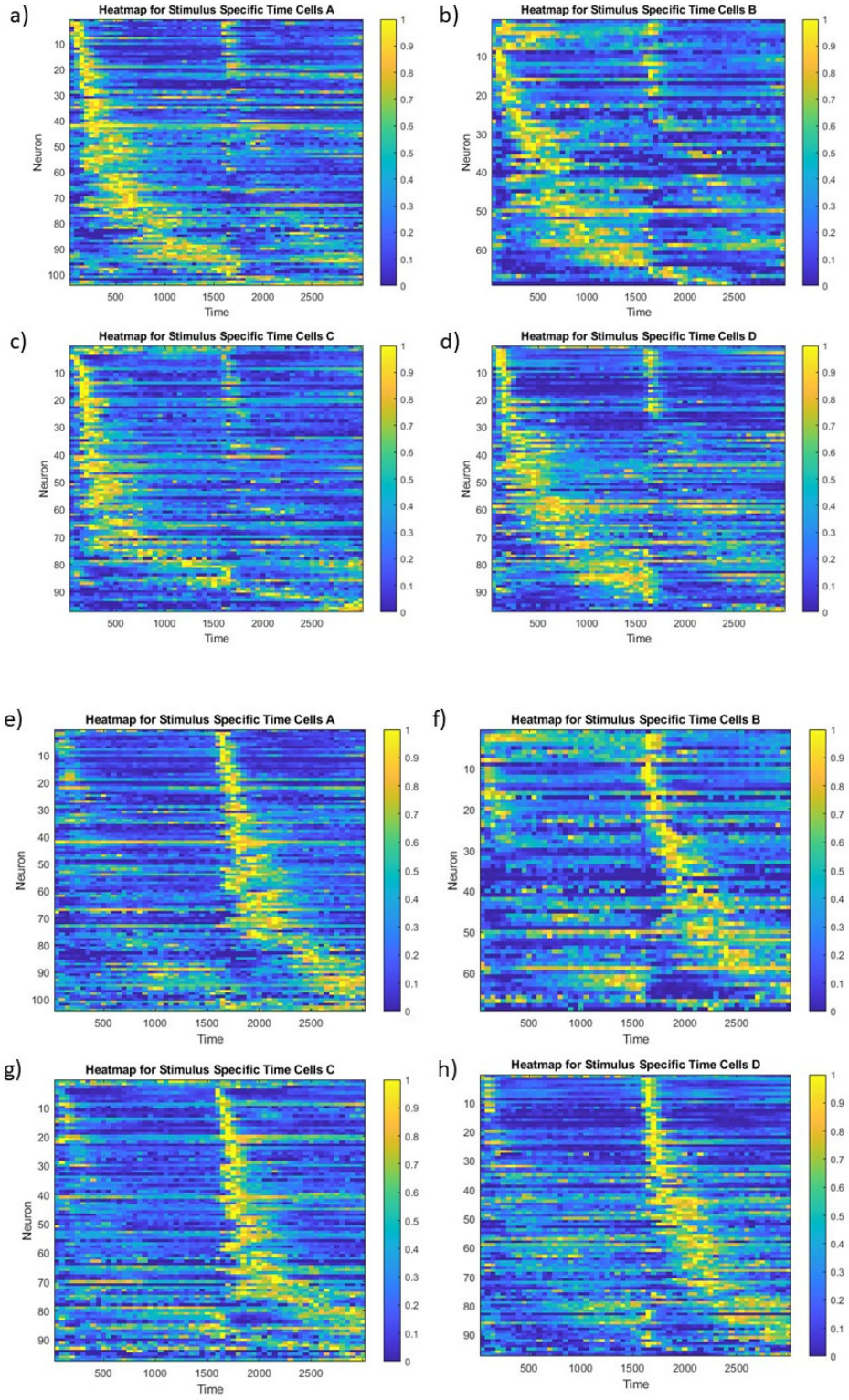
a)
Heatmap for Stimulus Specific Time Cells A
b)
Heatmap for Stimulus Specific Time Cells B
c)
Heatmap for Stimulus Specific Time Cells C
d)
Heatmap for Stimulus Specific Time Cells D
e)
Heatmap for Stimulus Specific Time Cells A
f)
Heatmap for Stimulus Specific Time Cells B
g)
Heatmap for Stimulus Specific Time Cells C
h)
Heatmap for Stimulus Specific Time Cells D
Neuron
Time

Figure 2.4: Heat maps for stimulus specific time cells by preferred stimulus. Cells are divided into their strongest stimulus as defined by the maximum stimulus coefficient. In a-d heat maps are plotted for cells that are specific to each stimulus, but only for trials in which that stimulus is presented in the first presentation period. In e-h heat maps are plotted for cells that are specific to each stimulus, but only for trials in which that stimulus is presented in the second presentation period. Taken together, these figures show that the stimulus specific cells fire to their preferred stimulus in either presentation position.

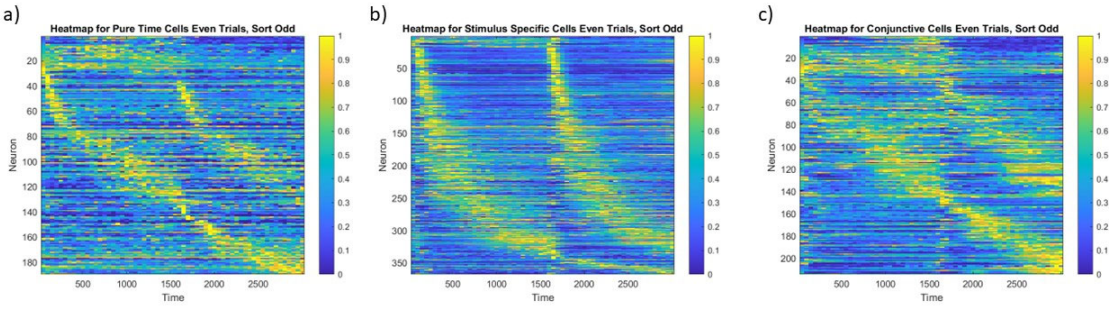

Figure 2.5: Averaged heat maps are consistent across even and odd trials. a-c) Firing from odd trials is selected for the pure time cells (a), stimulus specific time cells (b), and conjunctive time cells (c), and then rows are sorted by the "mu" value of the model fit for the even trials only. This shows coherence between firing on odd and even trials.

Conjunctive Time Cells

Conjunctive time cells are cells that fire to a specific list presentation, or combination of a specific pairs of stimulus 1 and 2 identities (ex. C followed by A). Figure 4a shows a heat map of these cells. Many of the conjunctive cells fire after the presentation of the second stimulus. These cells also encode information about the first stimulus after the presentation of the second stimulus, because they fire to a specific pair of stimuli. Ordinal position is also explicitly encoded in the list pair. Figures 2.6 b-d show examples of these cells at early (b), middle (c), and late (d) times within the trial.

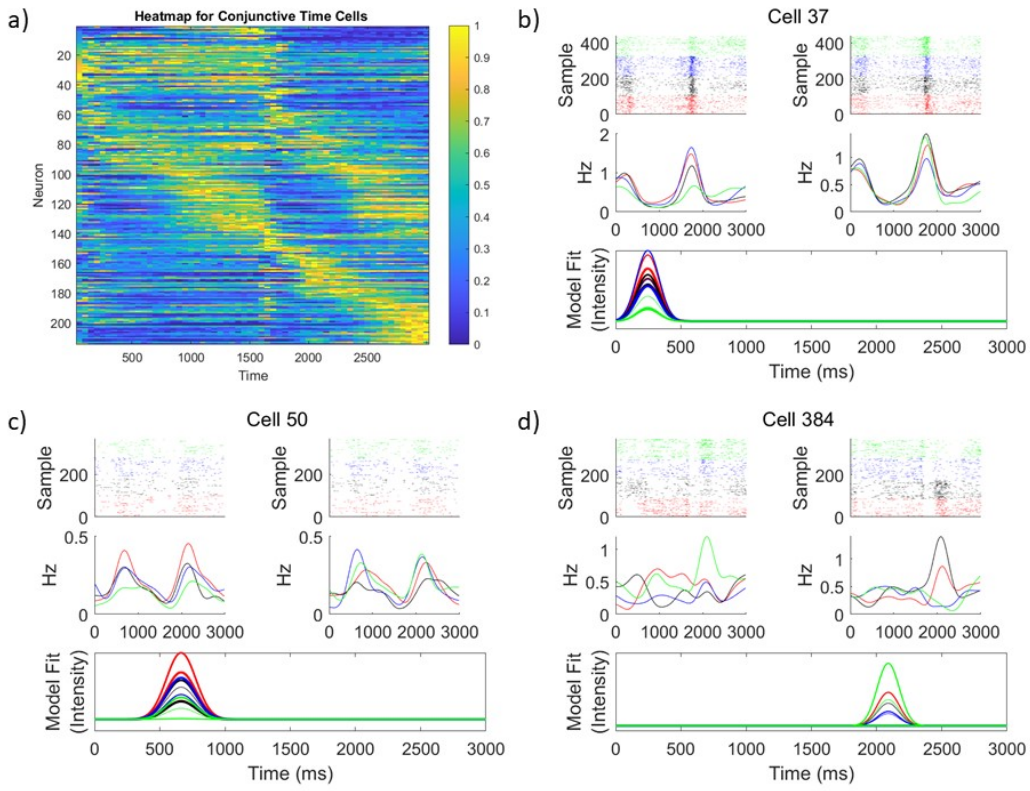

Figure 2.6: Single units best fit by the conjunctive time cell model. a) A heat map shows that the conjunctive time cells, which are selective to a particular combination of 1st and 2nd stimulus identities, tile the entirety of the delay with punctate fields. Each row represents the normalized firing of a neuron. Neurons are sorted by the model mu value of the conjunctive model fit. b-d) Examples of rasters for conjunctive cells show variation in firing over time. Samples are color-coded by and sorted by stimulus 1 identity on the left, and stimulus 2 identity on the right (trials where stimulus A are shown are in red, stimulus B in black, stimulus C in blue, and stimulus D in green.) The top panel shows rasters where each row represents a trial, and each line marks times the cell fired within that trial. The second panel is the Gaussian smoothed firing rate, calculated separately for each stimulus identity. The bottom panel shows the model fit of the conjunctive model. In this graph the colors of the lines represent the identity of the first stimulus (red= A, black=B, blue=C, green = D), and the width of the line represents the identity of the second stimulus (moving from thinnest to thickest from A to D). For example, a model that predicts activity for the condition of stimulus B presented first followed by stimulus A would be represented by a thin black line.

We also investigated the relationship between the mu and sigma values for the conjunctive cell population. For conjunctive time cells the linear and piecewise models were very similar, and the best fit model differed based on the criterion used (ΔAIC= 0.5, and ΔBIC= -6.2).

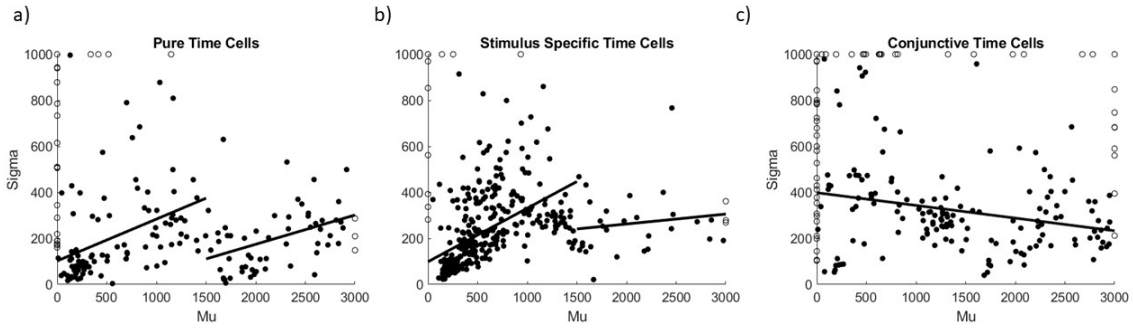

Figure 2.7: The relationship between the time field peak and width is non-linear. Scatter plots of the mu and sigma values of the model fits show the relationship between the time field peak time and the width, for all three subpopulations: a) pure time cells, b) stimulus specific time cells, and c) conjunctive time cells. In a and b, black lines show split linear models for two temporal epochs: the first spanning the first stimulus presentation period from 0-1500ms, the second spanning the second stimulus presentation period from 1500-3000ms. In c, the linear model is displayed showing the linear model extending from 0-3000ms.The unfilled black circles show cells with model fit values at a boundary, and these weren't included in the regression analyses.

In order to determine the source of the stimulus one information that persists past the presentation of the second stimulus, we combined the individual cell analyses with the decoders. Utilizing the three distinct subpopulations of cells: pure time cells, stimulus-specific time cells, and conjunctive time cells, we used the stimulus classifier on each cell type independently. Comparing results for cells with equivalent training and test times, shows significant differences for the ability to classify the identity of the first stimulus identity during the second presentation period, as compared to the ability to

classify the identity of the second stimulus during the first presentation time, for time bins 4 and 6 ($p < 0.01$), for the pure time cells. For the stimulus specific and conjunctive subpopulations, the classification of the first stimulus during the second presentation period was better than the classification of the second stimulus during the first presentation period was significantly better ($p<0.01$) for all 6 time bins. The full characteristics of the classifier can be seen in Figure 2.8.

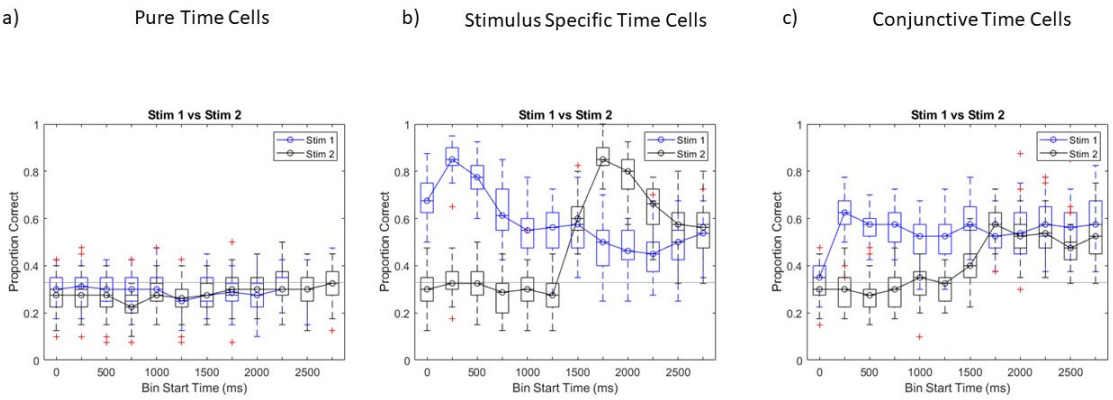

Figure 2.8: Stimulus specific and conjunctive time cells can decode the identity of the first stimulus after the presentation of the second. Utilizing the stimulus classifier on a) pure time cells, b) stimulus specific time cells and c) conjunctive time cells, the ability to decode the stimulus 1 and stimulus 2 identity was examined at all time points. Boxplots represent the median, and interquartile range of the decoding accuracies. Blue represents decoding of the first stimulus. Black represents decoding of the second stimulus. Significant ($p < 0.01$) stimulus 1 information is available after the presentation of stimulus 2 at 1500ms at all 6 delays for the stimulus specific and conjunctive subpopulations.

Discussion

During presentation of the second item in the list, the firing of ensembles in PFC carried information about what happened when at both positions during the list. The identity of the first item from the list could be robustly decoded throughout the entire list (Fig 1). The time within the study list could also be decoded (Fig 2.1).

However, because the time between the first and second item was fixed across trials it is not possible to distinguish timing information of the first item after the second item was presented. Analyses of single units showed that the population carried information about time via consistent firing profiles. The pure time model with Gaussian temporal firing fields better fit the data than a constant model for the overwhelming majority of cells (792/867). Although some neurons showed temporal profiles that were more complex than Gaussian receptive fields (see Fig 2.2, 2.3, 2.4), nonetheless the population demonstrated sequential firing, in that different neurons fire reliably at distinct points in the delay interval. This can also be seen by noting that the mu parameter, describing the peak time of firing, took a wide range of values across units.

Notably, stimulus information and temporal information were intimately related. This can be seen from the cross-temporal classifier, which showed a strong dynamic profile (Fig 2.2) and the broad distribution of temporal parameters for each of the subpopulations of neurons (Fig 2.5).

Stimulus Information

The population showed robust stimulus coding for the most recently-presented item throughout the duration of list presentation (Fig 1). To assess the form of stimulus coding we constructed three subpopulations of cells. These subpopulations are a convenience for understanding the data that depend on choices of the experimenter; they should not be taken to be an argument that there are distinct biologically-meaningful categories of cells. Nonetheless, these artificial subpopulations revealed several properties of the ensemble coding.

Consistent with previous analyses of these data (Rigotti et al., 2013), the single unit analysis showed many neurons that code for conjunctions of list items (the conjunctive subpopulation Fig. 2.4). In addition, there was also a substantial number of neurons that showed simple coding for the most recently-presented item (the stimulus-specific subpopulation, Fig. 2.3). The ``pure time'' subpopulation, by construction, showed less stimulus coding than the other two subpopulations (by choosing a more stringent threshold between the populations we could have turned down the amount of residual stimulus information in the pure time subpopulation).

The subset of the pure time subpopulation that peaked after 1500 ms suggests that some neurons may be sensitive to serial position in addition to conjunctions of items. Notably, because the identity of the first list item was able to be decoded after 1500 ms from the conjunctive subpopulation, these neurons cannot simply be responding to serial position X time X current item.

Temporal Information

As in many previous studies (Bright et al., 2020; Cruzado et al., 2020; Kraus et al., 2013; Tiganj et al., 2018), the accuracy of temporal information decayed in precision with the passage of time since the most recently presented item. This can be seen by noting the decrease in the accuracy of the time decoder (Fig 2.1) and in the curvature of the heatmaps (Figs. 2.2, 2.3, and 2.4). In the time following presentation of an item these plots show a reflected-J pattern. This indicates that the unfolding of the sequence ``slows'' with the passage of physical time in that the number of cells that begin firing at a time T after the stimulus goes down with T. This result is broadly

consistent with the decrease in the spanning dimension of a neural ensemble with the passage of time (Cueva et al., 2020). The increase in the spread of firing fields with mu (Fig 5) is also consistent with a decrease in temporal accuracy with the passage of time. Both of these properties are characteristic of time cells described in PFC (Cruzado et al., 2020; Tiganj et al., 2018) and other brain regions (Cao et al., 2021).

However, unlike previous findings, there appears to be a discontinuity in the sequences triggered by the first list item when the second list item was presented. This can be seen as a vertical line around 1500 ms in the heat maps (Figs 2.2, 2.3, and 2.4) and as an apparent discontinuity in the sigma/mu plots (Fig 2.5). One way to understand this finding is that the presentation of the second item in the list not only initiates a new sequence, but disrupts the ongoing sequence. The identity of the previous item is preserved in the ensemble, largely due to conjunctive coding (Fig 2.6) but the sequence it triggered is terminated. It is unclear whether these results would also hold if the timing between the first and second item was variable across trials or if it was important to perform the task. There is good evidence that the timing of preceding events is preserved in other brain regions and other tasks. For instance, Tsao et al., (2018) showed that ramping neurons in rodent LEC triggered by the initiation of a session in an open field persisted throughout the session, despite periodic contextual changes. Recording from rodent hippocampus, Shahbaba et al. (2022) showed long sequences of firing during study of a five item list and were able to decode time within the entire list. However, because the list was consistent across trials, it is unclear whether sequences from early items were terminated or not by subsequent items.

Future work should explore how multiple past events that vary in their identity and timing are represented in working memory in various brain regions.

CHAPTER THREE

Introduction

Previous research has tended to follow separate tracks for reward learning and learning of aversive experiences. However, these two forms of learning involve similar regions and processes, particularly in the hippocampus. Additionally, in "real-life" learning, these experiences are often interwoven and not discrete events. We sought to develop a task suitable for electrophysiological recordings that would allow investigators to interrogate how individual neurons generalize or separate these experiences when they are recorded simultaneously. Specifically, this task will combine these lines of research with that of time cells, which are known to tile the delay between experiences and thought to allow for the building of relationships between these stimuli. Animals were trained to associate a pair of tones with a water reward following a delay, and another pair of tones with an aversive outcome.

The experimental paradigm is designed to allow one to answer the question: if animals are trained to learn that tones predict a rewarding or aversive outcome following a predictable delay, do time cells in dorsal CA1 fire in patterns that are specific to valence of the outcome? For the data presented in this thesis, animals were implanted and then trained on the behavioral task. We will show that three rats were able to successfully learn the task presented. However, electrophysiological data had low cell yield and was unable to replicate previous findings on time cells. As this is possibly due to undetermined technical errors, I will focus on showing that the animals were able to learn

the task, and present avenues for future research. For sample rasters of identified cells, see Appendix, figures A1-A3.

Methods

Subjects

Three adult male Long Evans rats were used in this study. Animals were food and water restricted during weekdays, but were given ad libitum access to water for at least one hour following behavioral testing, and allowed free access to food and water on weekends. Their weight was maintained at 85% of free-feeding weight, or approximately 400 grams, and body condition score was also monitored daily. Animals were singly housed and lived on a 12-hour light/ dark cycle. This experiment was conducted during the animal's light cycle. Environmental enrichment was provided in cages in the form of wooden chew toys. All procedures were approved by the Boston University Institutional Animal Care and Use Committee.

Behavioral Apparatus

The behavioral apparatus consisted of a 12.7 x 30.5 cm wooden platform with four 40.6 cm high walls, at a slight outward angle, to keep the animal within the enclosure. A 1.0 cm diameter water port was centered approximately 2.5 cm above the floor on the front wall of the maze. A 1.0 cm diameter air puff port was located *2.5* cm above the water port of the front wall. Four tones were generated using Matlab scripts, at 1200 Hz, 1700 Hz, 3000 Hz and 7000 Hz. The rest session was conducted in a bucket with a 17 3/8-inch diameter and 12-inch height, topped with the same type of bucket

upside down with the bottom cut out (Fortex Industries). Animals were also given the opportunity to explore a “playground” which consisted of an open field with various rotating enrichment items multiple times a week.

Behavioral Training

Two weeks after arriving animals began being handled and exposed to the “playground” environment with a littermate. After acclimating, animals were implanted with tetrode drives in dorsal CA1, and singly housed to prevent damage to the drives. Upon recovery, animals were trained to discriminate between two tones, of which one signaled that a water reward would be delivered and one signaled that an air puff would be delivered at the same location. There was a 1s delay between the end of the tone and the delivery of the water/ air puff. Once rats were consistently licking the port on water trials and turning their head away and abstaining from licking the port on air trials, the second pair of tones was introduced. Once they learned both pairs separately, all four were presented pseudo randomly. Once this occurred the length of the delay was increased up to 4 seconds.

Session accuracy was calculated to determine if the animal was ready to move on to the next session type (from the first pair to the second pair or from the second pair to the combined pairs). Trials were scored as correct or incorrect via live video feed. Engaging with the water port was considered correct for water trials and incorrect for air trials, and not engaging with the water port was correct for air trials and incorrect for water trials. Trials where the animal was grooming and disengaged from the task were excluded. Ambiguous trials were also excluded. The final accuracy for a session is

calculated as the percent correct of trials in which the animal was engaged. Animals participated in 3 sessions of 60 trials per day, and there was a “rest” session after each training session where the animal was placed in the sleep chamber.

Surgical Methods

Animals were anesthetized with 5% isoflurane. They received injections of buprenorphine and cefazolin in accordance with IACUC protocols before surgery, and every 12 hours following surgery. The animal's head was shaved from approximately between the eyes to the ears, and then the skin was cleaned. An incision was made from the eyes to the mid-point between the ears, and the skull was exposed. Ground and stabilizing screws were inserted around the top of the skull. A craniotomy was drilled at approximately 2.8 AP and 2.4 ML from bregma. After the dura was removed the drive was lowered into the craniotomy and affixed to the skull using dental cement. Before the animal was removed from anesthesia, tetrodes were driven approximately 1 mm into the brain. Animals were monitored following IACUC protocols during recovery.

Histology

Following experiments, animals were anesthetized using 5% isoflurane. They were then given an intraperitoneal injection of Euthasol, and perfused using phosphate-buffered saline and formalin. After perfusion, the animal was decapitated and the brain was extracted. The brain was then placed in formalin, before being flash-frozen in a bath of 2-methylbutane and stored at -80 degrees. It was later sliced into 30 micrometer slices

using a cryostat, and then Nissl stained. Images were taken of the stained slices to approximate the locations of the tetrodes.

Statistical Methods

For each rat, trials were first excluded where the rat was not engaged or behavior was ambiguous. For learning of the first pair, learning was divided into the first 300 trials and the last 300 trials. Each of these segments was compared using a two proportions z-test (Illowsky & Dean, 2013). They were also then compared to a chance distribution. This process was repeated for the second pair. The combined task, in which both pairs were presented, was also compared to chance using two proportions z-test.

Results

We show that animals can learn an association task in which four tones predict a positive or negative outcome. For three animals that performed the entirety of the task, they learned the first pair in 75, 67, and 40 sessions of training, and the second pair faster in 21, 21, and 8 sessions of additional training (paired $t(2)=6.8$, $p<0.05$). They were then moved onto longer delays. Each animal showed variation in attention which could be reflected in accuracy. To account for the variations in attention to the task, only trials where the animal was engaged in the task (ie. not grooming) were counted towards the final accuracy. Figure 3.1a shows the increase in the number of correct trials to number of trials for each of the animals. Figure 3.1d takes the first 300 trials of first pair sessions and compares it to the last 300 trials of the first pair sessions where the animal is approaching the “learning” criteria. Using a two proportions z-test (Illowsky & Dean,

2013) for the early and late sessions the rats perform significantly better ($p < 0.01$) for the last 300 trials of learning as compared to the first 300 trials of learning (Rat 1, z= -12.9, Rat 2, z= -2.6, Rat 3, z= -4.2). Rat 1 did not perform significantly better than chance at first, but did at the end of training (early, z= 4.4, late, z= –8.9). Rats 2 and 3 perform significantly better than chance for both the first 300 trials and the last 300 trials (Rat 2 early, z= –3.1, Rat 2 late, z = -5.7, Rat 3 early, z= -4.3, Rat 3 late, z= -8.4).

After the animals learned the first pair, they were presented with a new pair of tones that signaled an upcoming water reward or aversive air puff. They were able to learn the new pair quickly. Figure 3.1 shows the learning of the second pair with respect to the number of trials performed, and figure 3.1e compares the number of correct trials for the first 300 and last 300 trials. Rats 1 and 2 performed significantly better ($p < 0.01$) for the last 300 trials than the first 300 trials (Rat 1, z= -5.2, Rat 2, z= -7.3). For Rats 1 and 2, performance was significantly better than chance for both early and late (Rat 1 early, z= -3.2, Rat 1 late, z = -10.2, Rat 2 early, z= -5.6, Rat 2 late, z = -10.5). For Rat 3 performance did not reliably change (z = 1.3) although both early and late were significantly better than chance (early, z= -9.9, late, z= -8.8). Figure 3.1c compares the trajectory of learning for each pair. Comparing the performance for the first 300 trials between the first pair of tones and the second pair of tones, all rats showed better performance for the second pair (Rat 1, z= -7.7, Rat 2, z= -2.5, Rat 3 z= -5.9).

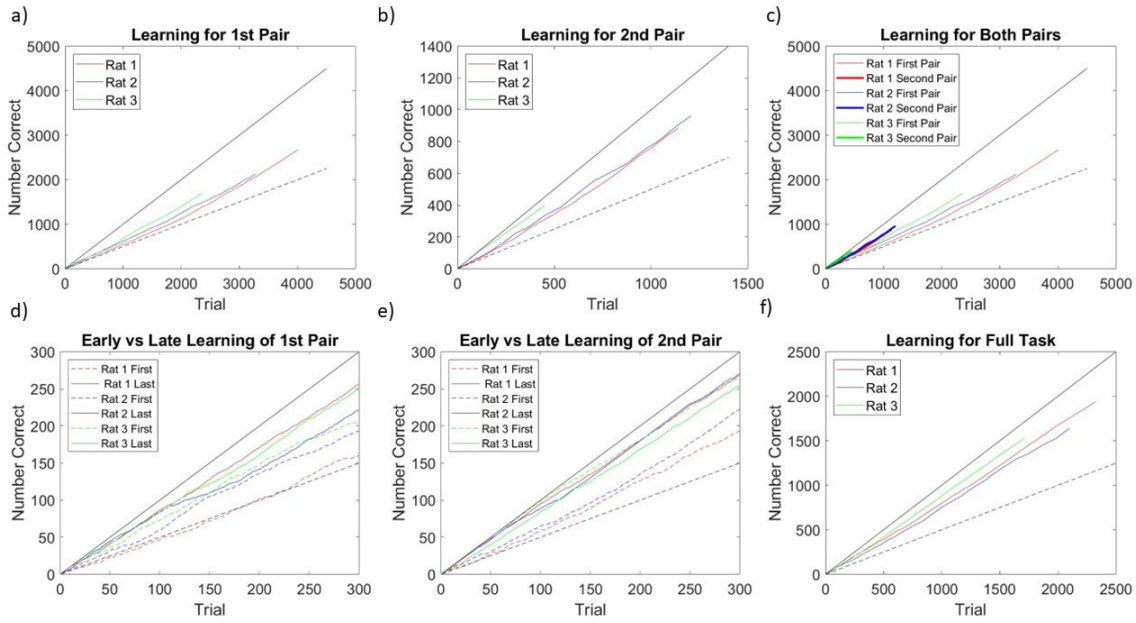

Figure 3.1: Animals learned to respond to tones that predict different outcomes. a) Animals obtain more correct rewards for the number of trials performed with experience. The number correct on the y-axis represents the number of trials that were labeled as correctly licking on reward trials or correctly moving away from the port on air puff trials. In all graphs, blue represents the performance of rat 1, red represents the performance of rat 2, and yellow represents the performance of rat 3. The solid black line represents what would be seen from perfect performance, the dashed black line represents what would be expected from chance (50%) performance in all graphs. b) Correct trials as a function of trials performed for each rat for the second pair presented. Trials on the x-axis count the total number of trials the animal has participated in. The number correct on the y-axis represents the number of trials that were labeled as correctly licking on reward trials or correctly moving away from the port on air puff trials. c) Comparing the number of trials for the first pair of learning to the second pair of learning. Thin lines represent learning for the first pair and thick lines represent learning for the second pair. d) Two critical sections of the learning curve presented in a. The dashed lines show the number correct for the number of trials for the first 300 trials. The solid lines show the number correct for the number of trials for the last 300 trials of learning. We see that there is an increase in the number of correct trials per trials completed as the animals learn the associations. e) Two critical sections of the learning curve presented in b. The dashed lines show the number correct for the number of trials for the first 300 trials. The solid lines show the number correct for the number of trials for the last 300 trials of learning. We see that there is an increase in the number of correct trials per trials completed as the animals learn the associations. f) Animals learn the combined task in which both pairs are intermingled.

Upon learning each pair, animals were able to quickly combine the information to complete the four tone task, as seen in figure 3.1f. Within the first 300 trials all animals were performing significantly above chance, (Rat 1, $z= -6.8$, Rat 2, $z= -4.1$, Rat 3, $z= -6.3$). This difference shows the animals are able to perform this four tone task, critical for differentiating valence and tone identity.

Discussion

We showed that rats are able to learn a behavioral task that combines positive and negative stimuli and has the potential to be suitable for electrophysiological recordings. Animals learned the task; all animals were better at performing the first pair at the end of training than at the beginning. For 2 out of 3 animals, performance improved between early and late trials for the 2nd pair, and for the 3rd rat performance remained high throughout learning of the second pair. As shown above and in Figure 3.1c, the learning rate was faster and number of sessions required to learn the second pair was less than the number of sessions required to learn the first. Animals were able to assemble knowledge about the two pairs into the four tone task which is suitable for recordings.

This study is limited by the number of animals that were used. Increasing the number of animals and including female animals would allow for greater confidence in the generalizability of the results, and the ability to investigate any sex differences. Additionally, the interpretation of the behavioral results is limited by the accuracy of the human scoring. Finally, the valence and the reaction are confounded so it is impossible to disentangle valence and motor planning.

This task shows the ability to examine the underpinnings of how positive and negative memories are encoded. The information regarding neural encoding in the absence of disease could be used to further our understanding of diseases of memory such as PTSD and Alzheimer's Disease.

CHAPTER FOUR

Summary of Findings

We first showed that working memory in the prefrontal cortex holds stimulus information beyond the presentation of subsequent stimuli. This stimulus information is held in time cells, that contradict predictions of persistent firing (Goldman-Rakic, 1995; Lundqvist et al., 2018). Finally, this experiment showed a discontinuity appears at the presentation of the second stimulus that cannot be seen in single delay experiments (Cao et al., 2021; Cruzado et al., 2020). Indeed, the width of the fields seems to reset at the presentation of the new stimuli. This supports theories of mixed selectivity (Fusi et al., 2016; Rigotti et al., 2013) in which prefrontal neurons code for multiple task dimensions, in this case stimulus, serial position, and continuous time.

We next developed a task in which the animals are trained to discriminate four tones that predict either a positive or a negative outcome. Animals showed final performance above chance and initial performance. The task shows promise for future electrophysiological recordings.

Limitations of the Current Work

The current work is limited by the low number of animals. While this is prudent from the perspective of reducing animal participants, it makes it impossible to identify any sex differences. Additionally, all animals in the valence task were male. Recent work has shown no sex differences in performance of temporal and order learning (Jayachandran et al., 2022; Reeders et al., 2021). However, there are sex differences in

fear memory (Baran et al., 2009; Day & Stevenson, 2020; Finkelstein et al., 2022; Lovick & Zangrossi, 2021), that could affect the encoding of the stimuli in the valence task. Additionally, inclusion of more animals would help to increase confidence in the generalizability of these results.

Additionally, the tasks contain consistent delays between the stimulus presentation and the outcome. Particularly for the recollection of list task, the consistency of the delay makes it impossible to dissociate continuous time from serial position. Future work would be required to determine if cells are firing at a long delay from the initiation of the trial, or at a short delay after the presentation of the second stimulus.

A further challenge for this work, and most similar studies, is the dependence on "over-trained" animals. Additionally, their experience outside of the task is relatively sparse. This repetition is required practically in order to record sufficient trials for statistical analysis. However, it raises questions about the applicability of the neural mechanisms of this learning to more "real world" examples. In all of these studies the animal has an expectation of what information is required (or not required), to achieve its goals, while in real life this may be more ambiguous. Additionally, these tasks provide stimuli across a consistent time course. This could allow the animal to parse temporal information onto a known temporal structure. For example, in the list task, the animal may be aware that the presentation of the second stimulus is halfway between the presentation of the first stimulus and the decision point. This could allow the neural code to "anchor" itself in ways that would not be possible in an unstructured environment.

Theoretical Implications

This work falsifies the hypothesis that stimulus information is carried exclusively in persistent firing cells (Constantinidis et al., 2018; Goldman-Rakic, 1995). There is clear stimulus information in cells that are also temporally modulated. Additionally, we have shown that some stimulus information persists past the presentation of additional stimuli in both a conjunctive manner and in the representation of single stimuli. Finally, we have extended previous work on time cells (Cruzado et al., 2020; Kraus et al., 2013; MacDonald et al., 2011, 2013; Mau et al., 2018; Pastalkova et al., 2008; Tiganj et al., 2017, 2018) to include the presentation of multiple items. We have also shown that many time cells fire at the same time irrespective of serial position.

Previous work has identified a linear relationship between peak firing time and field width in a single delay (Cao et al., 2021; Cruzado et al., 2020). We have shown that the relationship between the peak firing time and the field width is discontinuous at the point of the second presentation period, exhibiting an apparent "resetting" of the signal. This could be accounted for by previous models (such as Howard et al., 2014) by adding a conjunctive term, in which cells fire conjunctively to a particular time point and serial position.

Future Directions

This work has made a critical step forward in time cell research by interrogating the effect of a second stimulus on time cell sequences. Future directions include

expanding memory tasks to include longer lists of stimuli. This would help to move the experimental paradigm towards more “real life” situations in which stimuli come forth in longer lists than pairs.

Importantly, in this task the variables of time and serial position are perfectly confounded. This makes it impossible to dissociate if those cells that fire later in the trial (after 1500ms) are firing at a prolonged delay to the presentation of the first stimulus, or to a conjunction of time and the second serial position. Further experiments could utilize a variable delay to dissociate serial position and time.

While these experiments would be fairly straightforward to implement (as much as conducting new experiments can be), a more difficult problem to tackle is determining the effect of overtraining on representations of time. Some of this can be rectified by looking at learning data. However, performance on the task is typically low as the animals are just learning, and there is often a small number of learning trials to sample from.

The behavioral task could be improved upon in future iterations using three main approaches. The first proposed modification is to automate the lick port. Using a laser beam at the lick port to determine if the animal is licking or avoiding the port. This would be more consistent and replicable than using manual behavioral scoring. The lick port could be further mechanized by implementing a vacuum in the water reward tray. Quickly removing the water reward would force the animal to respond promptly to the reward, which could improve temporal precision. A second possible modification to the task would be to implement running on the treadmill during the delay period. This would

keep the animal engaged in the task (ie. prevent grooming), and hold behavior consistent during the delay (for examples see Kraus et al., 2013; Mau et al., 2018; Salz et al., 2016). This stability would eliminate the possibility that changes in movement and spatial location are driving changes in firing. However, it is currently unknown if animals can maintain performance with the addition of the treadmill. The third improvement proposed is to expand the task to 8 tones. An expansion to 8 tones would allow the dissociation of reward value and spatial location. Two tones could predict a positive outcome at location A and 2 tones could predict a positive outcome at location B. Two more tones could predict a negative outcome at location A, and a final 2 could predict a negative outcome at location B. It is currently unknown if rats could learn the 8 tone task, and if possible, training likely would be time intensive. However, if it is possible, the use of 8 tones would help to decorrelate reward and spatial location.

Future work could include the use of tetrode recordings in dorsal CA1 of the hippocampus. These could test various hypotheses about how the hippocampus encodes information during this task. First, one could determine if time cells are found in this paradigm, and how they compare to time cells in established paradigms. To do this, one could additionally train animals to run a delayed alternation task with a treadmill delay. This behavioral paradigm would serve as a good control to the valence testing task as multiple studies have recorded time cells using delayed alternation (Kraus et al., 2013; Pastalkova et al., 2008).

If time cells are identified in the opposing valence paradigm, one could further determine if those time cells are stimulus specific and/ or stimulus modulated. This would

be expected based on previous work in the hippocampus (Cruzado et al., 2020; Shahbaba et al., 2022; Terada et al., 2017). Possible outcomes include 1) no temporal coding, 2) time cells that fire across all stimuli 3) time cells that fire to a single stimulus 4) time cells that fire to stimuli of the same valence 5) a combination of cells that meet criteria for different subtypes (1-4). We hypothesized that we would identify some cells from all subtypes, and will classify individual cells based on a maximum likelihood model that will fit temporal and stimulus parameters (*GitHub - tcnlab/maxlikespy*). The proportions of cells that fit into each category could be measured and in future work could be compared to other regions that have been implicated in integrating stimulus and valence information, such as ventral hippocampus (Komorowski et al., 2013; Shpokayte et al., 2020) and the amygdala (Paton et al., 2006). Additionally, linear classifiers can be used to compare the ability to decode the stimulus and the ability to decode the valence based on cellular activity patterns. This is another quantitative measure to determine which type of coding is more prevalent in this region.

The inclusion of 3 sessions per day allows for two advantages when combined with successful recording: 1) It allows for cells to be analyzed over more trials than a rat will perform in a single session and 2) It could allow one to answer the question if stimulus specificity, time fields, and/ or valence remap across sessions in dorsal CA1. The remapping of place cells has been previously identified (Colgin et al., 2008; Kinsky et al., 2018; Muller & Kubie, 1987; Quirk et al., 1990). However, systematic investigation into remapping time cells has yet to be undertaken, despite theory supporting similar properties of the coding of both dimensions (Howard et al., 2014).

Additionally, fear conditioning, and later extinction, have been shown to cause remapping of place cells (Moita et al., 2004; Wang et al., 2015). The effect of fear conditioning on stability is contentious, and may be modulated by experimental conditions and behavioral paradigm (Schuette et al., 2020; Wang et al., 2013). Combining this research with the finding that separate populations of cells encode positive and negative experiences in the ventral hippocampus (Shpokayte et al., 2020), yields the question of if and how time cells remap, and what the effect of outcome is on that remapping.

Finally, one could evaluate the impact of stress on generalization and remapping of mild positive and negative stimuli. Stress has been shown to impact fear conditioning and generalization (Akirav et al., 2009; Bender et al., 2018; Kausche et al., 2021; Rau et al., 2005; Trow et al., 2019). Importantly, this process is hormonally modulated (Jackson et al., 2006; Peyrot et al., 2020). However, generalization has been shown to be modulated by intensity of the fear stimulus (Dunsmoor et al., 2009; Ghosh & Chattarji, 2014). Previous work has focused on behavioral generalization (Dunsmoor et al., 2009), or firing in areas such as the amygdala (Ghosh & Chattarji, 2014). To implement this, two groups of animals, containing both males and females, would need to be trained on the task. The first could then undergo a single prolonged stress paradigm prior to learning. This would allow the researcher to contrast the generalization of encoding positive and negative stimuli between the traumatized and control groups in dorsal hippocampus, another critical part of the learning circuit.

This research has added new information as to mechanisms for how neurons encode a multi-dimensional world. Its limitations open up possible avenues for future research. The field of memory research remains an exciting new horizon, with implications for basic science and psychiatric disease.

APPENDIX

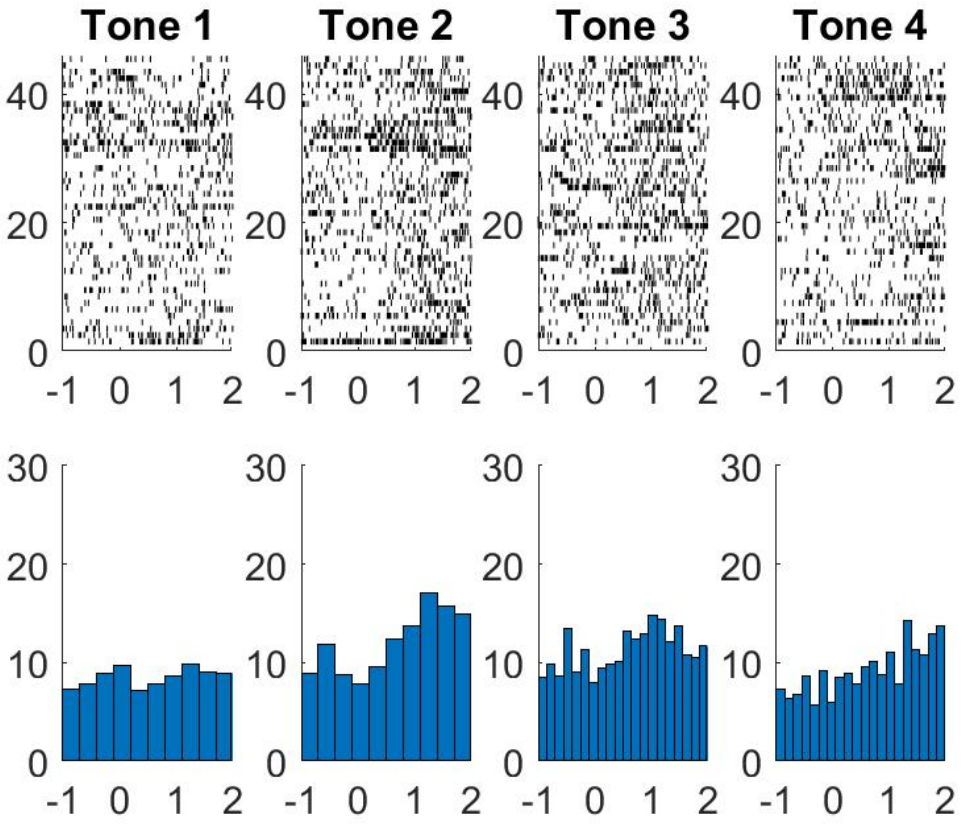

Figure A.1: Sample Cell Raster. A sample cell recorded from the task described in Chapter 3. Top row shows a raster plot for the cell. Trials are divided by the tone played for that trial, and consolidated across the 3 sessions for the day. Zero marks the tone onset, and 1 second marks the end of the delay period, and the onset of the outcome. Bottom row shows a perievent stimulus time historgram, representing the averaged firing rates across the trials.

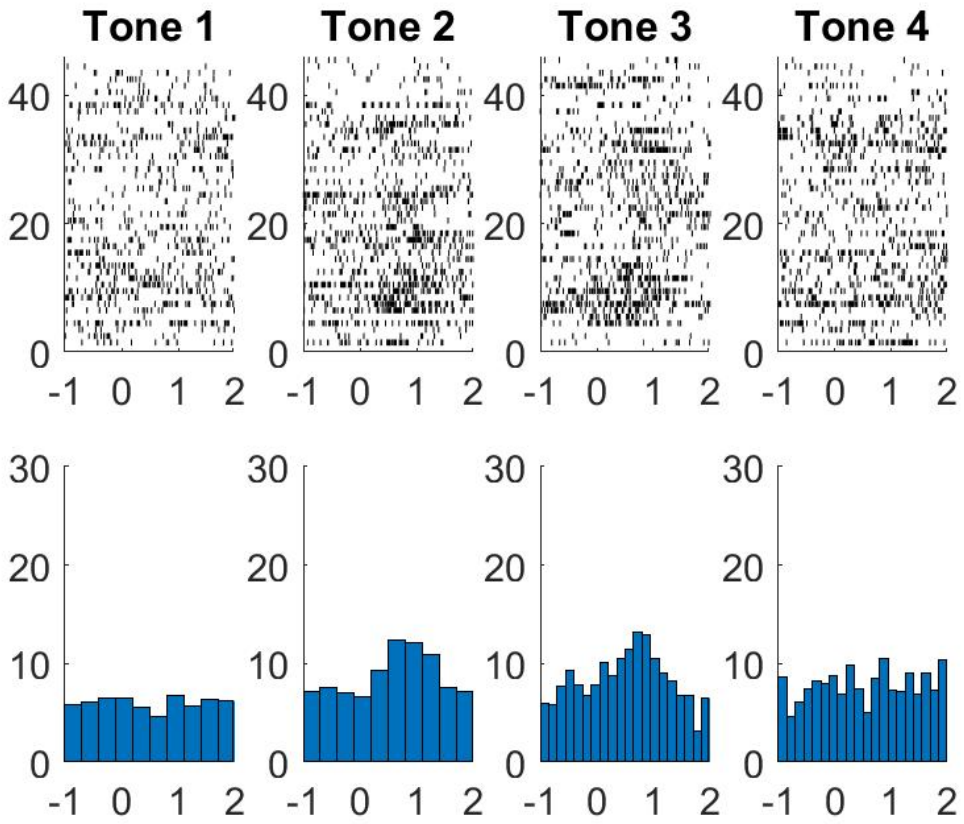

Figure A.2: Sample Cell Raster. A sample cell recorded from the task described in Chapter 3. Top row shows a raster plot for the cell. Trials are divided by the tone played for that trial, and consolidated across the 3 sessions for the day. Zero marks the tone onset, and 1 second marks the end of the delay period, and the onset of the outcome. Bottom row shows a perievent stimulus time historgram, representing the averaged firing rates across the trials.

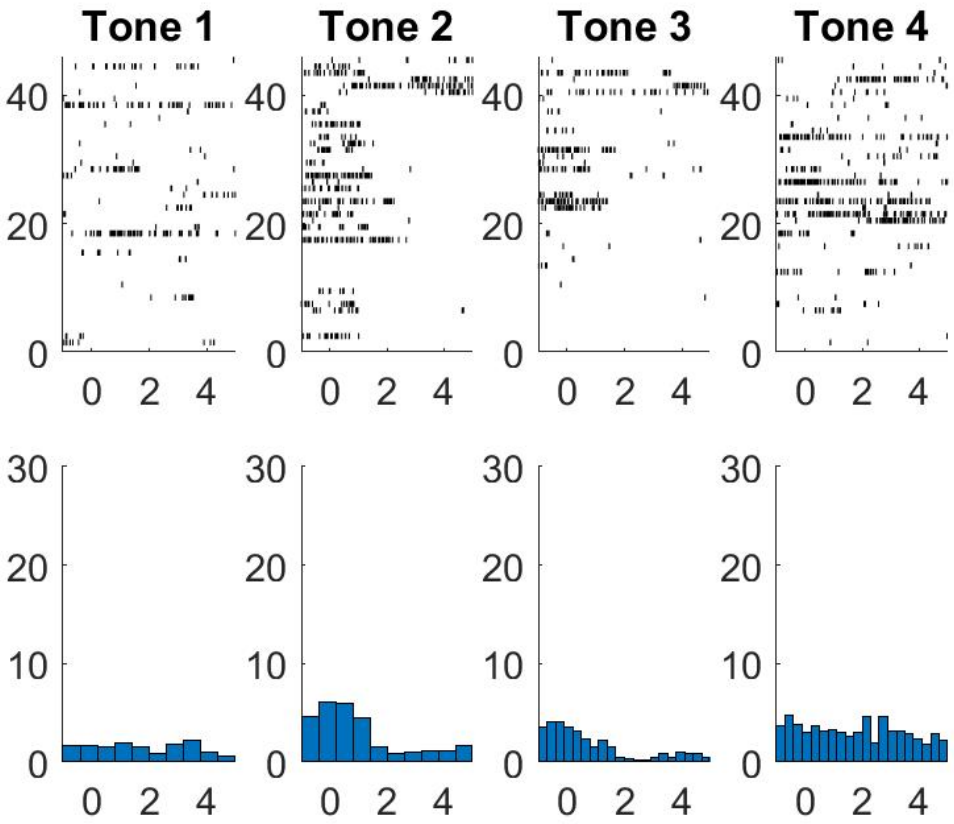

Figure A.3: Sample Cell Raster. A sample cell recorded from the task described in Chapter 3. Top row shows a raster plot for the cell. Trials are divided by the tone played for that trial, and consolidated across the 3 sessions for the day. Zero marks the tone onset, and 4 seconds marks the end of the delay period, and the onset of the outcome. Bottom row shows a perievent stimulus time histogram, representing the averaged firing rates across the trials.

BIBLIOGRAPHY

Akhlaghpour, H., Wiskerke, J., Choi, J. Y., Taliaferro, J. P., Au, J., & Witten, I. B. (2016). Dissociated sequential activity and stimulus encoding in the dorsomedial striatum during spatial working memory. *ELife*, *5*, e19507. https://doi.org/10.7554/eLife.19507

Akirav, I., Segev, A., Motanis, H., & Maroun, M. (2009). D-Cycloserine into the BLA reverses the impairing effects of exposure to stress on the extinction of contextual fear, but not conditioned taste aversion. *Learning and Memory*, *16*(11), 682–686. https://doi.org/10.1101/LM.1565109

Alexander, A. S., Carstensen, L. C., Hinman, J. R., Raudies, F., William Chapman, G., & Hasselmo, M. E. (2020). Egocentric boundary vector tuning of the retrosplenial cortex. *Science Advances*, *6*(8). https://doi.org/10.1126/SCIADV.AAZ2322/SUPPL_FILE/AAZ2322_SM.PDF

Amaral, D. G., & Witter, M. P. (1989). The three-dimensional organization of the hippocampal formation: A review of anatomical data. *Neuroscience*, *31*(3), 571–591. https://doi.org/10.1016/0306-4522(89)90424-7

Anderson, M. I., & Jeffery, K. J. (2003). *Heterogeneous modulation of place cell firing by changes in context. 23*(26), 8827–8835.

Atkinson, R. C., & Shiffrin, R. M. (1968). Human memory: A proposed system and its control processes. In K. W. Spence & J. T. Spence (Eds.), *The Psychology of Learning and Motivation* (Vol. 2, pp. 89–105). Academic Press.

Baddeley, A. D., & Hitch, G. J. (1974). Working memory. In G. H. Bower (Ed.), *The psychology of learning and motivation: Advances in research and theory* (Vol. 8, pp. 47–90). Academic Press.

Baran, S. E., Armstrong, C. E., Niren, D. C., Hanna, J. J., & Conrad, C. D. (2009). Chronic stress and sex differences on the recall of fear conditioning and extinction. *Neurobiology of Learning and Memory*, *91*(3), 323–332. https://doi.org/10.1016/J.NLM.2008.11.005

Bender, C. L., Otamendi, A., Calfa, G. D., & Molina, V. A. (2018). Prior stress promotes the generalization of contextual fear memories: Involvement of the gabaergic signaling within the basolateral amygdala complex. *Progress in Neuro-Psychopharmacology and Biological Psychiatry*, *83*, 18–26. https://doi.org/10.1016/J.PNPBP.2017.12.003

Bright, I. M., Meister, M. L. R., Cruzado, N. A., Tiganj, Z., Buffalo, E. A., & Howard, M. W. (2020). A temporal record of the past with a spectrum of time constants in the

monkey entorhinal cortex. *Proceedings of the National Academy of Sciences of the United States of America*, *117*(33), 20274–20283. https://doi.org/10.1073/PNAS.1917197117

Brincat, S. L., & Miller, E. K. (2015). Frequency-specific hippocampal-prefrontal interactions during associative learning. *Nature Neuroscience*, *18*(4), 576–581. https://doi.org/10.1038/nn.3954

Brown, G. D. A., Preece, T., & Hulme, C. (2000). Oscillator-based memory for serial order. *Psychological Review*, *107*(1), 127–181.

Cao, R., Bladon, J. H., Charczynski, S. J., Hasselmo, M. E., & Howard, M. W. (2021). Internally Generated Time in the Rodent Hippocampus is Logarithmically Compressed. *BioRxiv*, 2021.10.25.465750. https://doi.org/10.1101/2021.10.25.465750

Cavanagh, S. E., Towers, J. P., Wallis, J. D., Hunt, L. T., & Kennerley, S. W. (2018). Reconciling persistent and dynamic hypotheses of working memory coding in prefrontal cortex. *Nature Communications*, *9*(1), 1–16.

Colgin, L. L., Moser, E. I., & Moser, M. B. (2008). Understanding memory through hippocampal remapping. *Trends in Neurosciences*, *31*(9), 469–477. https://doi.org/10.1016/J.TINS.2008.06.008

Constantinidis, C., Funahashi, S., Lee, D., Murray, J. D., Qi, X. L., Wang, M., & Arnsten, A. F. T. (2018). Persistent Spiking Activity Underlies Working Memory. *Journal of Neuroscience*, *38*(32), 7020–7028. https://doi.org/10.1523/JNEUROSCI.2486-17.2018

Cromer, J. A., Roy, J. E., & Miller, E. K. (2010). Representation of Multiple, Independent Categories in the Primate Prefrontal Cortex. *Neuron*, *66*(5), 796–807. https://doi.org/10.1016/j.neuron.2010.05.005

Cruzado, N. A., Tiganj, Z., Brincat, S. L., Miller, E. K., & Howard, M. W. (2020). Conjunctive representation of what and when in monkey hippocampus and lateral prefrontal cortex during an associative memory task. *Hippocampus*, *30*(12), 1332–1346. https://doi.org/10.1002/hipo.23282

Cueva, C. J., Saez, A., Marcos, E., Genovesio, A., Jazayeri, M., Romo, R., Salzman, C. D., Shadlen, M. N., & Fusi, S. (2020). Low-dimensional dynamics for working memory and time encoding. *Proceedings of the National Academy of Sciences of the United States of America*, *117*(37), 23021–23032. https://doi.org/10.1073/PNAS.1915984117

Day, H. L. L., & Stevenson, C. W. (2020). The neurobiological basis of sex differences in

learned fear and its inhibition. *The European Journal of Neuroscience*, *52*(1), 2466. https://doi.org/10.1111/EJN.14602

De Santi, S., de Leon, M. J., Rusinek, H., Convit, A., Tarshish, C. Y., Roche, A., Tsui, W. H., Kandil, E., Boppana, M., Daisley, K., Wang, G. J., Schlyer, D., & Fowler, J. (2001). Hippocampal formation glucose metabolism and volume losses in MCI and AD. *Neurobiology of Aging*, *22*(4), 529–539. https://doi.org/https://doi.org/10.1016/S0197-4580(01)00230-5

Denny, C. A., Lebois, E., & Ramirez, S. (2017). From Engrams to Pathologies of the Brain. *Frontiers in Neural Circuits*, *11*, 23. https://doi.org/10.3389/fncir.2017.00023

Dunsmoor, J. E., Mitroff, S. R., & LaBar, K. S. (2009). Generalization of conditioned fear along a dimension of increasing fear intensity. *Learning & Memory*, *16*(7), 460–469. https://doi.org/10.1101/lm.1431609

Dunsmoor, Joseph E, Campese, V. D., Ceceli, A. O., LeDoux, J. E., & Phelps, E. A. (2015). Outcome in place of an expected threat diminishes recovery of defensive responses. *Biological Psychiatry*, *78*(3), 203–209. https://doi.org/10.1016/j.biopsych.2014.12.008

Eichenbaum, H. (2013). Memory on time. In *Trends in Cognitive Sciences*. https://doi.org/10.1016/j.tics.2012.12.007

Eichenbaum, H. (2014). Time cells in the hippocampus: A new dimension for mapping memories. *Nature Reviews Neuroscience*, *15*(11), 732–744. https://doi.org/10.1038/NRN3827

Eichenbaum, H. (2017). Prefrontal–hippocampal interactions in episodic memory. *Nature Reviews Neuroscience*, *18*(9), 547–558. https://doi.org/10.1038/nrn.2017.74

Eliav, T., Maimon, S., Aljadeff, J., Tsodyks, M., Ginosar, G., Las, L., & Ulanovsky, N. (2021). Multiscale representation of very large environments in the hippocampus of flying bats. *Science*, *372*(6545), eabg4020. https://doi.org/10.1126/science.abg4020

Farovik, A., Place, R. J., Mckenzie, S., Porter, B., Munro, C. E., & Eichenbaum, H. (2015). *Behavioral/Cognitive Orbitofrontal Cortex Encodes Memories within Value-Based Schemas and Represents Contexts That Guide Memory Retrieval*. https://doi.org/10.1523/JNEUROSCI.0134-15.2015

Fechner , Boring, Edwin Garrigues,, Howes, Davis H., G. T. (1966). *Elements of psychophysics.* Holt, Rinehart and Winston.

Fenton, A. A., Kao, H.-Y., Neymotin, S. A., Olypher, A., Vayntrub, Y., Lytton, W. W., & Ludvig, N. (2008). Unmasking the CA1 ensemble place code by exposures to

small and large environments: more place cells and multiple, irregularly arranged, and expanded place fields in the larger space. *The Journal of Neuroscience : The Official Journal of the Society for Neuroscience*, *28*(44), 11250–11262. https://doi.org/10.1523/JNEUROSCI.2862-08.2008

Finkelstein, A. B., Eloïse Leblanc, H., Cole, R. H., Gallerani, T., Vieira, A., Zaki, Y., & Ramirez, S. (2022). *Social reactivation of fear engrams enhances memory recall*. https://doi.org/10.1073/pnas

Funahashi, S., Bruce, C. J., & Goldman-Rakic, P. S. (1989). Mnemonic coding of visual space in the monkey's dorsolateral prefrontal cortex. *Journal of Neurophysiology*, *61*(2), 331–349. https://doi.org/10.1152/JN.1989.61.2.331

Fusi, S., Miller, E. K., & Rigotti, M. (2016). Why neurons mix: high dimensionality for higher cognition. *Current Opinion in Neurobiology*, *37*, 66–74. https://doi.org/10.1016/j.conb.2016.01.010

Fuster, J. M., & Alexander, G. E. (1971). Neuron Activity Related to Short-Term Memory. *New Series*, *173*(3997), 652–654.

Gauthier, J. L., & Tank, D. W. (2018). A Dedicated Population for Reward Coding in the Hippocampus. *Neuron*, *99*(1), 179-193.e7. https://doi.org/10.1016/J.NEURON.2018.06.008)

Ghosh, S., & Chattarji, S. (2014). Neuronal encoding of the switch from specific to generalized fear. *Nature Neuroscience*, *18*(1), 112–120. https://doi.org/10.1038/nn.3888

Gilbertson, M. W., Shenton, M. E., Ciszewski, A., Kasai, K., Lasko, N. B., Orr, S. P., & Pitman, R. K. (2002). Smaller hippocampal volume predicts pathologic vulnerability to psychological trauma. *Nature Neuroscience*, *5*(11), 1242–1247. https://doi.org/10.1038/nn958

Gill, P. R., Mizumori, S. J. Y., & Smith, D. M. (2011). Hippocampal episode fields develop with learning. *Hippocampus*, *21*(11), 1240–1249. https://doi.org/10.1002/HIPO.20832

Girardeau, G., Inema, I., & Buzsáki, G. (2017). Reactivations of emotional memory in the hippocampus–amygdala system during sleep. *Nature Neuroscience 2017 20:11*, *20*(11), 1634–1642. https://doi.org/10.1038/nn.4637

GitHub - tcnlab/maxlikespy. (n.d.). Retrieved October 11, 2021, from https://github.com/tcnlab/maxlikespy

Goh, W. Z. (2022). *Remembering the past to predict the future: a scale-invariant timeline*

for memory and anticipation. [Doctoral Dissertatoin, Boston University]. Boston University Theses & Dissertations.

Golden, S. A., Covington, H. E., Berton, O., & Russo, S. J. (2011). A standardized protocol for repeated social defeat stress in mice. *Nature Protocols*, *6*(8), 1183–1191. https://doi.org/10.1038/nprot.2011.361

Goldman-Rakic, P. S. (1995). Cellular basis of working memory. In *Neuron* (Vol. 14, Issue 3, pp. 477–485). https://doi.org/10.1016/0896-6273(95)90304-6

Hacker, M. J. (1980). *Speed and accuracy of recency judgments for events in short-term memory. 15*, 846–858.

Haider, S., Batool, Z., & Rafiq, S. (2020). Method for the identification of pharmacological intervention for the disruption of fear memory in PTSD-rat model. *MethodsX*, *7*. https://doi.org/10.1016/j.mex.2020.101059

Henson, R. N. A. (1998). Short-Term Memory for Serial Order: The Start-End Model. *Cognitive Psychology*, *36*(2), 73–137. https://doi.org/10.1006/COGP.1998.0685

Hollup, S. A., Molden, S., Donnett, J. G., Moser, M.-B., & Moser, E. I. (2001). *Accumulation of Hippocampal Place Fields at the Goal Location in an Annular Watermaze Task*.

Howard, M W, Shankar, K. H., Aue, W., & Criss, A. H. (2015). A distributed representation of internal time. *Psychological Review*, *122*(1), 24–53.

Howard, M W., MacDonald, C. J., Tiganj, Z., Shankar, K. H., Du, Q., Hasselmo, M. E., & Eichenbaum, H. (2014). A Unified Mathematical Framework for Coding Time, Space, and Sequences in the Hippocampal Region. *Journal of Neuroscience*, *34*(13), 4692–4707. https://doi.org/10.1523/JNEUROSCI.5808-12.2014

Illowsky, B., & Dean, S. (2013). *Introductory Statistics*. OpenStax.

Isserles, M., Tendler, A., Roth, Y., Bystritsky, A., Blumberger, D. M., Ward, H., Feifel, D., Viner, L., Duffy, W., Zohar, J., Keller, C. J., Bhati, M. T., Etkin, A., George, M. S., Filipcic, I., Lapidus, K., Casuto, L., Vaishnavi, S., Stein, A., … Ressler, K. J. (2021). Deep Transcranial Magnetic Stimulation Combined With Brief Exposure for Posttraumatic Stress Disorder: A Prospective Multisite Randomized Trial. *Biological Psychiatry*, *90*(10), 721–728. https://doi.org/10.1016/J.BIOPSYCH.2021.04.019

Jackson, E. D., Payne, J. D., Nadel, L., & Jacobs, W. J. (2006). Stress Differentially Modulates Fear Conditioning in Healthy Men and Women. *Biological Psychiatry*, *59*(6), 516–522. https://doi.org/10.1016/J.BIOPSYCH.2005.08.002

Jacobsen, C. F. (1936). Studies of cerebral function in primates. I. The functions of the frontal association areas in monkeys. *Comparative Psychology Monographs*, *13*, *3*, 1–60.

Jayachandran, M., Langius, P., Pazos Rego, F., Vertes, R. P., & Allen, T. A. (2022). Sex and estrous cycle in memory for sequences of events in rats. In *Behavioral Neuroscience* (p. No Pagination Specified-No Pagination Specified). American Psychological Association. https://doi.org/10.1037/bne0000508

Jin, D. Z., Fujii, N., & Graybiel, A. M. (2009). Neural representation of time in cortico-basal ganglia circuits. *Proceedings of the National Academy of Sciences*, *106*(45), 19156–19161.

Kahana, M. J. (1996). Associative retrieval processes in free recall. *Memory \& Cognition*, *24*, 103–109.

Kausche, F. M., Zerbes, G., Kampermann, L., Büchel, C., & Schwabe, L. (2021). Neural signature of delayed fear generalization under stress. *Psychophysiology*, *58*(11). https://doi.org/10.1111/PSYP.13917

Keene, C. S., Bladon, J., Mckenzie, S., Liu, C. D., O'keefe, J., & Eichenbaum, H. (2016). *Complementary Functional Organization of Neuronal Activity Patterns in the Perirhinal, Lateral Entorhinal, and Medial Entorhinal Cortices*. https://doi.org/10.1523/JNEUROSCI.4368-15.2016

Kentros, C. G., Agnihotri, N. T., Streater, S., Hawkins, R. D., & Kandel, E. R. (2004). Increased Attention to Spatial Context Increases Both Place Field Stability and Spatial Memory. *Neuron*, *42*(2), 283–295. https://doi.org/10.1016/S0896-6273(04)00192-8

Kinsky, N. R., Sullivan, D. W., Mau, W., Hasselmo, M. E., & Eichenbaum, H. B. (2018). Hippocampal Place Fields Maintain a Coherent and Flexible Map across Long Timescales. *Current Biology*, *28*(22), 3578-3588.e6. https://doi.org/10.1016/J.CUB.2018.09.037/ATTACHMENT/096E5932-0946-4A38-9732-A2BB3E132F39/MMC1.PDF

Komorowski, R. W., Garcia, C. G., Wilson, A., Hattori, S., Howard, M. W., & Eichenbaum, H. (2013). Ventral Hippocampal Neurons Are Shaped by Experience to Represent Behaviorally Relevant Contexts. *Journal of Neuroscience*, *33*(18), 8079–8087. https://doi.org/10.1523/JNEUROSCI.5458-12.2013

Komorowski, R. W., Manns, J. R., & Eichenbaum, H. (2009). Robust conjunctive item - Place coding by hippocampal neurons parallels learning what happens where. *Journal of Neuroscience*, *29*(31), 9918–9929. https://doi.org/10.1523/JNEUROSCI.1378-09.2009

Kraus, B. J., Brandon, M. P., Robinson, R. J., Connerney, M. A., Hasselmo, M. E., & Eichenbaum, H. (2015). During running in place, grid cells integrate elapsed time and distance run. *Neuron*, *88*(3), 578–589. https://doi.org/10.1016/j.neuron.2015.09.031

Kraus, B. J., Robinson, R. J., White, J. A., Eichenbaum, H., & Hasselmo, M. E. (2013). Hippocampal "time cells": Time versus path integration. *Neuron*, *78*(6), 1090–1101. https://doi.org/10.1016/j.neuron.2013.04.015

Kraus, Benjamin J., Robinson, R. J. 2nd, White, J. A., Eichenbaum, H., & Hasselmo, M. E. (2013). Hippocampal "time cells": time versus path integration. *Neuron*, *78*(6), 1090–1101. https://doi.org/10.1016/j.neuron.2013.04.015

Lantrip, C. (2021). Combining Transcranial Magnetic Stimulation With Behavioral Interventions for Posttraumatic Stress Disorder: Reasons for Optimism Despite Negative Findings. *Biological Psychiatry*, *90*(10), e43–e44. https://doi.org/10.1016/j.biopsych.2021.09.003

LeDoux, J. (2015). *Anxious.* Oneworld Publications. http://public.ebookcentral.proquest.com/choice/publicfullrecord.aspx?p=2126068

Liberzon, I., Krstov, M., & Young, E. A. (1997). Stress-restress: Effects on ACTH and fast feedback. *Psychoneuroendocrinology*, *22*(6), 443–453. https://doi.org/10.1016/S0306-4530(97)00044-9

Liu, X., Ramirez, S., Pang, P. T., Puryear, C. B., Govindarajan, A., Deisseroth, K., & Tonegawa, S. (2012). Optogenetic stimulation of a hippocampal engram activates fear memory recall. *Nature*, *484*(7394), 381–385. https://doi.org/10.1038/nature11028

Lovick, T. A., & Zangrossi, H. (2021). Effect of Estrous Cycle on Behavior of Females in Rodent Tests of Anxiety. *Frontiers in Psychiatry*, *12*, 1492. https://doi.org/10.3389/FPSYT.2021.711065/BIBTEX

Lundqvist, M., Herman, P., & Miller, E. K. (2018). Working Memory: Delay Activity, Yes! Persistent Activity? Maybe Not. *The Journal of Neuroscience*, *38*(32), 7013 LP – 7019. https://doi.org/10.1523/JNEUROSCI.2485-17.2018

MacDonald, C. J., Carrow, S., Place, R., & Eichenbaum, H. (2013). Distinct Hippocampal Time Cell Sequences Represent Odor Memories in Immobilized Rats. *Journal of Neuroscience*, *33*(36), 14607–14616. https://doi.org/10.1523/jneurosci.1537-13.2013

MacDonald, C. J., Lepage, K. Q., Eden, U. T., & Eichenbaum, H. (2011). Hippocampal "time cells" bridge the gap in memory for discontiguous events. *Neuron*, *71*(4),

737–749. https://doi.org/10.1016/j.neuron.2011.07.012

Mau, W., Sullivan, D. W., Kinsky, N. R., Hasselmo, M. E., Howard, M. W., & Eichenbaum, H. (2018). The Same Hippocampal CA1 Population Simultaneously Codes Temporal Information over Multiple Timescales. *Current Biology : CB*, *28*(10), 1499-1508.e4. https://doi.org/10.1016/J.CUB.2018.03.051

McKenzie, S., Frank, A. J., Kinsky, N. R., Porter, B., Rivière, P. D., & Eichenbaum, H. (2014). Hippocampal representation of related and opposing memories develop within distinct, hierarchically organized neural schemas. *Neuron*, *83*(1), 202–215. https://doi.org/10.1016/J.NEURON.2014.05.019/ATTACHMENT/C8BF4B8A-6F2B-4113-BCE9-07E713AD6886/MMC1.PDF

Mello, G. B. M., Soares, S., & Paton, J. J. (2015). A scalable population code for time in the striatum. *Current Biology*, *25*(9), 1113–1122.

Miller, E. K., & Cohen, J. D. (2001). An Integrative Theory of Prefrontal Cortex Function. *Annual Review of Neuroscience*, *24*(1), 167–202. https://doi.org/10.1146/annurev.neuro.24.1.167

Miller, E. K., Li, L., & Desimone, R. (1991). A neural mechanism for working and recognition memory in inferior temporal cortex. *Science*, *254*(5036), 1377–1379. https://doi.org/10.1126/SCIENCE.1962197

Miracle, A. D., Brace, M. F., Huyck, K. D., Singler, S. A., & Wellman, C. L. (2006). Chronic stress impairs recall of extinction of conditioned fear. *Neurobiology of Learning and Memory*, *85*(3), 213–218. https://doi.org/10.1016/j.nlm.2005.10.005

Moita, M. A. P., Rosis, S., Zhou, Y., LeDoux, J. E., & Blair, H. T. (2004). Putting Fear in Its Place: Remapping of Hippocampal Place Cells during Fear Conditioning. *Journal of Neuroscience*, *24*(31), 7015–7023. https://doi.org/10.1523/JNEUROSCI.5492-03.2004

Muller, R. U., & Kubie, J. L. (1987). The effects of changes in the environment on the spatial firing of hippocampal complex-spike cells. *The Journal of Neuroscience*, *7*(7), 1951 LP – 1968. https://doi.org/10.1523/JNEUROSCI.07-07-01951.1987

Murray, J. D., Bernacchia, A., Roy, N. A., Constantinidis, C., Romo, R., & Wang, X.-J. (2017). Stable population coding for working memory coexists with heterogeneous neural dynamics in prefrontal cortex. *Proceedings of the National Academy of Sciences*, *114*(2), 394–399. https://doi.org/10.1073/pnas.1619449114

Nieh, E. H., Schottdorf, M., Freeman, N. W., Low, R. J., Lewallen, S., Koay, S. A., Pinto, L., Gauthier, J. L., Brody, C. D., & Tank, D. W. (2021). Geometry of abstract learned knowledge in the hippocampus. *Nature*, 1–5.

O'Keefe, J, & Burgess, N. (1996). *Geometric determinants of the place fields of hippocampal neurons*. *381*(6581), 425–428.

O'Keefe, J, & Dostrovsky, J. (1971). The hippocampus as a spatial map. Preliminary evidence from unit activity in the freely-moving rat. *Brain Research*, *34*(1), 171–175. https://doi.org/10.1016/0006-8993(71)90358-1

O'Keefe, John, & Burgess, N. (2005). Dual phase and rate coding in hippocampal place cells: theoretical significance and relationship to entorhinal grid cells. *Hippocampus*, *15*(7), 853–866. https://doi.org/10.1002/HIPO.20115

Öngür, D., & Price, J. L. (2000). The Organization of Networks within the Orbital and Medial Prefrontal Cortex of Rats, Monkeys and Humans. *Cerebral Cortex*, *10*(3), 206–219. https://doi.org/10.1093/CERCOR/10.3.206

Pastalkova, E., Itskov, V., Amarasingham, A., & Buzsáki, G. (2008). Internally Generated Cell Assembly Sequences in the Rat Hippocampus. *Science*, *321*(5894), 1322–1327. https://doi.org/10.1126/science.1159775

Pastalkova, Eva, Itskov, V., Amarasingham, A., & Buzsáki, G. (2008). Internally Generated Cell Assembly Sequences in the Rat Hippocampus. *Science*, *321*(5894), 1322–1327. https://doi.org/10.1126/SCIENCE.1159775

Paton, J. J., Belova, M. A., Morrison, S. E., & Salzman, C. D. (2006). The primate amygdala represents the positive and negative value of visual stimuli during learning. *Nature*, *439*(7078), 865–870. https://doi.org/10.1038/nature04490

Peyrot, C., Brouillard, A., Morand-Beaulieu, S., & Marin, M. F. (2020). A review on how stress modulates fear conditioning: Let's not forget the role of sex and sex hormones. *Behaviour Research and Therapy*, *129*, 103615. https://doi.org/10.1016/J.BRAT.2020.103615

Phillips, R. G., & LeDoux, J. E. (1992). Differential contribution of amygdala and hippocampus to cued and contextual fear conditioning. *Behavioral Neuroscience*, *106*(2), 274–285. https://doi.org/10.1037//0735-7044.106.2.274

Quirk, G. J., Muller, R. U., & Kubie, J. L. (1990). The firing of hippocampal place cells in the dark depends on the rat's recent experience. *Journal of Neuroscience*, *10*(6), 2008–2017. https://doi.org/10.1523/JNEUROSCI.10-06-02008.1990

Ramirez, S., Liu, X., Lin, P.-A., Suh, J., Pignatelli, M., Redondo, R. L., Tomás, R. L., & Tonegawa, S. (2013). Creating a False Memory in the Hippocampus. *Science*, *341*(6144), 387–391. https://doi.org/10.1126/science.1239073

Ramirez, S., Liu, X., MacDonald, C. J., Moffa, A., Zhou, J., Redondo, R. L., &

Tonegawa, S. (2015). Activating positive memory engrams suppresses depression-like behaviour. *Nature*, *522*(7556), 335–339. https://doi.org/10.1038/nature14514

Rau, V., DeCola, J. P., & Fanselow, M. S. (2005). Stress-induced enhancement of fear learning: An animal model of posttraumatic stress disorder. *Neuroscience & Biobehavioral Reviews*, *29*(8), 1207–1223. https://doi.org/10.1016/J.NEUBIOREV.2005.04.010

Redondo, R. L., Kim, J., Arons, A. L., Ramirez, S., Liu, X., & Tonegawa, S. (2014). Bidirectional switch of the valence associated with a hippocampal contextual memory engram. *Nature*, *513*(7518), 426–430. https://doi.org/10.1038/nature13725

Reeders, P. C., Hamm, A. G., Allen, T. A., & Mattfeld, A. T. (2021). Medial prefrontal cortex and hippocampal activity differentially contribute to ordinal and temporal context retrieval during sequence memory. *Learning and Memory*, *28*(4), 134–147. https://doi.org/10.1101/LM.052365.120

Rich, P. D., Liaw, H.-P., & Lee, A. K. (2014). Large environments reveal the statistical structure governing hippocampal representations. *Science (American Association for the Advancement of Science)*, *345*(6198), 814–817. https://doi.org/10.1126/science.1255635

Rigotti, M., Barak, O., Warden, M. R., Wang, X.-J., Daw, N. D., Miller, E. K., & Fusi, S. (2013). The importance of mixed selectivity in complex cognitive tasks. *Nature*, *497*(7451), 585–590. https://doi.org/10.1038/nature12160

Robinson, N. T. M., Descamps, L. A. L., Russell, L. E., Buchholz, M. O., Bicknell, B. A., Antonov, G. K., Lau, J. Y. N., Nutbrown, R., Schmidt-Hieber, C., & Häusser, M. (2020). Targeted Activation of Hippocampal Place Cells Drives Memory-Guided Spatial Behavior. *Cell*, *183*(6), 1586-1599.e10. https://doi.org/10.1016/J.CELL.2020.09.061

Robinson, N. T. M., Priestley, J. B., Rueckemann, J. W., Garcia, A. D., Smeglin, V. A., Marino, F. A., & Eichenbaum, H. B. (2017). Medial entorhinal cortex selectively supports temporal coding by hippocampal neurons. *Neuron*, *94*(3), 677. https://doi.org/10.1016/J.NEURON.2017.04.003

Rossi-Pool, R., Zizumbo, J., Alvarez, M., Vergara, J., Zainos, A., & Romo, R. (2019). Temporal signals underlying a cognitive process in the dorsal premotor cortex. *Proceedings of the National Academy of Sciences*, *116*, 7523–7532.

Salz, D. M., Tiganj, Z., Khasnabish, S., Kohley, A., Sheehan, S., Howard, M. W., & Eichenbaum, H. (2016). Time Cells in Hippocampal Area CA3. *Journal of Neuroscience*, *36*(28), 7476–7484. https://doi.org/10.1523/jneurosci.0087-16.2016

Schiller, D., Monfils, M.-H., Raio, C. M., Johnson, D. C., Ledoux, J. E., & Phelps, E. A. (2010). Preventing the return of fear in humans using reconsolidation update mechanisms. *Nature*, *463*(7277), 49–53. https://doi.org/10.1038/nature08637

Schuette, P. J., Reis, F. M. C. V., Maesta-Pereira, S., Chakerian, M., Torossian, A., Blair, G. J., Wang, W., Blair, H. T., Fanselow, M. S., Kao, J. C., & Adhikari, A. (2020). Long-Term Characterization of Hippocampal Remapping during Contextual Fear Acquisition and Extinction. *Journal of Neuroscience*, *40*(43), 8329–8342. https://doi.org/10.1523/JNEUROSCI.1022-20.2020

Shahbaba, B., Li, L., Agostinelli, F., Saraf, M., Cooper, K. W., Haghverdian, D., Elias, G. A., Baldi, P., & Fortin, N. J. (2022). Hippocampal ensembles represent sequential relationships among an extended sequence of nonspatial events. *Nature Communications 2022 13:1*, *13*(1), 1–17. https://doi.org/10.1038/s41467-022-28057-6

Sheehan, D. J., Charczynski, S., Fordyce, B. A., Hasselmo, M. E., & Howard, M. W. (2021). "A compressed representation of spatial distance in the rodent hippocampus''. *BioRxiv*, 2021.02.15.431306. https://doi.org/10.1101/2021.02.15.431306

Shpokayte, M., McKissick, O., Yuan, B., Rahsepar, B., Fernandez, F. R., Ruesch, E., Grella, S. L., White, J. A., Liu, X. S., & Ramirez, S. (2020). Hippocampal cells multiplex positive and negative engrams. *BioRxiv*, 2020.12.11.419887. https://doi.org/10.1101/2020.12.11.419887

Sreenivasan, K. K., Curtis, C. E., & D'Esposito, M. (2014). Revisiting the role of persistent neural activity during working memory. *Trends in Cognitive Sciences*, *18*(2), 82–89. https://doi.org/https://doi.org/10.1016/j.tics.2013.12.001

Sreenivasan, K. K., & D'Esposito, M. (2019). The what, where and how of delay activity. *Nature Reviews Neuroscience*, *20*(8), 466–481. https://doi.org/10.1038/s41583-019-0176-7

Taxidis, J., Pnevmatikakis, E. A., Dorian, C. C., Mylavarapu, A. L., Arora, J. S., Samadian, K. D., Hoffberg, E. A., & Golshani, P. (2020). Differential Emergence and Stability of Sensory and Temporal Representations in Context-Specific Hippocampal Sequences. *Neuron*, *108*(5), 984-998.e9. https://doi.org/10.1016/J.NEURON.2020.08.028

Terada, S., Sakurai, Y., Nakahara, H., & Fujisawa, S. (2017). Temporal and Rate Coding for Discrete Event Sequences in the Hippocampus. *Neuron*, *94*(6), 1248-1262.e4. https://doi.org/10.1016/j.neuron.2017.05.024

Tiganj, Z., Cromer, J. A., Roy, J. E., Miller, E. K., & Howard, M. W. (2018).

Compressed Timeline of Recent Experience in Monkey Lateral Prefrontal Cortex. *Journal of Cognitive Neuroscience*, *30*(7), 935–950. https://doi.org/10.1162/JOCN_A_01273

Tiganj, Z., Gershman, S. J., Sederberg, P. B., & Howard, M. W. (2019). Estimating scale-invariant future in continuous time. *Neural Computation*, *31*(4), 681. https://doi.org/10.1162/NECO_A_01171

Tiganj, Z., Jung, M. W., Kim, J., & Howard, M. W. (2017). Sequential Firing Codes for Time in Rodent Medial Prefrontal Cortex. *Cerebral Cortex (New York, NY)*, *27*(12), 5663. https://doi.org/10.1093/CERCOR/BHW336

Trow, J. E., Jones, A. M., & McDonald, R. J. (2019). Comparison of the effects of repeated exposures to predictable or unpredictable stress on the behavioural expression of fear in a discriminative fear conditioning to context task. *Physiology & Behavior*, *208*, 112556. https://doi.org/10.1016/J.PHYSBEH.2019.05.017

Tsao, A., Sugar, J., Lu, L., Wang, C., Knierim, J. J., Moser, M.-B., & Moser, E. I. (2018). Integrating time from experience in the lateral entorhinal cortex. *Nature*, *561*(7721), 57–62. https://doi.org/10.1038/s41586-018-0459-6

Umbach, G., Kantak, P., Jacobs, J., Kahana, M., Pfeiffer, B. E., Sperling, M., & Lega, B. (2020). Time cells in the human hippocampus and entorhinal cortex support episodic memory. *Proceedings of the National Academy of Sciences*, *117*(45), 28463–28474. https://doi.org/10.1073/PNAS.2013250117

Uylings, H. B. M., Groenewegen, H. J., & Kolb, B. (2003). Do rats have a prefrontal cortex? *Behavioural Brain Research*, *146*(1–2), 3–17. https://doi.org/10.1016/J.BBR.2003.09.028

Wang, M. E., Fraize, N. P., Yin, L., Yuan, R. K., Petsagourakis, D., Wann, E. G., & Muzzio, I. A. (2013). Differential roles of the dorsal and ventral hippocampus in predator odor contextual fear conditioning. *Hippocampus*, *23*(6). https://doi.org/10.1002/hipo.22105

Wang, M. E., Yuan, R. K., Keinath, A. T., Álvarez, M. M. R., & Muzzio, I. A. (2015). Extinction of Learned Fear Induces Hippocampal Place Cell Remapping. *Journal of Neuroscience*, *35*(24), 9122–9136. https://doi.org/10.1523/JNEUROSCI.4477-14.2015

Warden, M. R., & Miller, E. K. (2010). Task-Dependent Changes in Short-Term Memory in the Prefrontal Cortex. *Journal of Neuroscience*, *30*(47), 15801–15810. https://doi.org/10.1523/JNEUROSCI.1569-10.2010

Wood, E R, Dudchenko, P. A., Robitsek, R. J., & Eichenbaum, H. (2000). Hippocampal

neurons encode information about different types of memory episodes occurring in the same location. *Neuron*, *27*(3), 623–633.

Wood, Emma R, Dudchenko, P. A., & Eichenbaum, H. (1999). *The Global Record of Memory in Hippocampal Neuronal Activity*. *397*, 613–616.

Xu, R., Hu, X., Jiang, X., Zhang, Y., Wang, J., & Zeng, X. (2020). Longitudinal volume changes of hippocampal subfields and cognitive decline in Parkinson's disease. *Quantitative Imaging in Medicine and Surgery*, *10*(1), 220.

Yehuda, R., & LeDoux, J. (2007). Response Variation following Trauma: A Translational Neuroscience Approach to Understanding PTSD. *Neuron*, *56*(1), 19–32. https://doi.org/https://doi.org/10.1016/j.neuron.2007.09.006

CURRICULUM VITAE